APPLIED SCIENCE DIVISION
Litton Systems, Inc.
2003 East Hennepin Avenue
Minneapolis, Minnesota 55413

INVESTIGATION OF SPUTTERING EFFECTS ON THE MOON'S SURFACE

Eighth Quarterly Status Report on
Contract NASw-751

Covering Period 25 January 1965 to 24 April 1965

Submitted to:

National Aeronautics and Space Administration Headquarters
Office of Lunar and Planetary Programs, Code SL
Washington, D.C. 20546

Prepared by:

G. K. Wehner
D. L. Rosenberg
C. E. KenKnight

Submitted by: G. K. Wehner

G. K. Wehner, Director
Surface Physics Laboratory

Report No.: 2792
Date: 14 May 1965
Project: 89308

TABLE OF CONTENTS

INVESTIGATION OF SPUTTERING EFFECTS ON THE MOON'S SURFACE

Eighth Quarterly Status Report
Contract NASw-751

ABSTRACT

29719

Measurements of photometric and polarimetric properties of sifted powder surfaces have been obtained for the materials greenstone and tektite for the particle size ranges 0-20, 20-44, 44-74, and 74-300μ in addition to earlier data for tholeiitic basalt and granodiorite. The surfaces were darkened by simulated solar-wind bombardment. The normal albedos and photometric function were measured in ultraviolet, green, and red light and indicated fair agreement with lunar measurements in the smaller size ranges after bombardment by the equivalent of 10^4 to 10^5 yr of solar-wind exposure. Two indices of the polarization of green light scattered from these rock powder surfaces were shown to increase equivalently with particle size. Comparison to lunar values of the polarization indices and albedo indicated that most of the particles in the lunar dust cover are less than 50 or 100μ in diameter if the unbombarded particles are opaque or translucent, respectively. Some uncertainty in this conclusion arises from the interpretation of the lunar albedo at zero phase angle.

author

I. INTRODUCTION

A paper titled "Simulated Solar-Wind Bombardment of Possible Lunar Surface Materials" was presented at the 46th Annual Meeting of the American Geophysical Union, 19-22 April, Washington, D.C., and was the subject of many subsequent private discussions. An abstract is given below. G. K. Wehner and C. E. KenKnight attended the Conference on the Nature of the Surface of the Moon, 15-16 April, Goddard Space Flight Center, Greenbelt, Maryland.

This report is concerned with the dependence of photometric and polarimetric properties of sifted, particulate surfaces upon particle size. It extends the data previously given[1] for tholeiitic basalt and granodiorite to greenstone and tektite for the particle size ranges 0-20, 20-44, 44-74, and 74-300μ. Photometric properties were obtained in three wavelength intervals. Corresponding polarization curves were obtained for green light and are here subject to analysis by two methods, of which the new method presented here is shown to be far preferable.

The results of an extensive photoelectric observation program by T. Gehrels have been reduced and published with great detail by Gehrels, Coffeen, and Owings.[2] A number of well-defined lunar regions were studied at many phases and at several wavelengths to obtain both photometric and polarimetric data. We have begun an analysis of these data in terms of the methods discussed in this report and preliminary indications are that their paper is of outstanding value in the understanding of the nature of the lunar surface.

Paper presented at the 46th Annual Meeting of the
American Geophysical Union, Washington, D.C.

Simulated Solar-Wind Bombardment of Possible Lunar Surface Materials

D. L. Rosenberg and C. E. KenKnight
Applied Science Division, Litton Systems, Inc.
Minneapolis, Minnesota 55413

ABSTRACT

Interpretation of lunar light-scattering data has been reconsidered, taking into account the solar-wind bombardment. Bombardment of the lunar surface has been simulated in a low-pressure, radio-frequency excited, hydrogen plasma discharge. Reflection curves, polarization curves, and normal albedos in several wavelength regions have been determined for sifted powder surfaces of a number of possible lunar materials. After as much as 10^5 simulated years of solar-wind bombardment, the surfaces exhibited decreased albedo and increased backscatter and polarization. The degree and nature of the change in photometric and polarimetric properties with bombardment depended on the material, its particle size, and its surface compaction. Materials rich in quartz required the longest times (10^5 simulated years) for albedos to be reduced to lunar values. Surfaces (particularly solid surfaces) of particles larger than 10^{-2} cm in diameter darkened by simulated solar-wind bombardment gave forward scatter and polarization greatly in excess of lunar values. This indicated a very complete lunar dust cover.

II. REFLECTION PROPERTIES OF ROCK POWDERS

The results presented in the Seventh Quarterly Status Report[1] have been extended to two more materials: greenstone and tektite.

Greenstone was chosen because our previous studies of a bombarded greenstone surface of only one particle size fraction indicated optical scattering properties in white light very similar to those of the moon. The present studies cover various bombardment doses and particle size fractions. The optical scattering of the surface is measured in several wavelength regions. Tektite material was studied because of its possible lunar origin. The tektites were obtained through the courtesy of Dr. John A. O'Keefe of Goddard Space Flight Center.

A. Greenstone

Surfaces of sifted greenstone, an altered metamorphic rock of possible basalt parentage, have been studied before bombardment and after the equivalent of 10^4 to 10^5 yr of solar-wind bombardment. Surfaces of particle size fraction 0-20, 20-44, 44-74, and 74-300μ were bombarded by hydrogen ions in an rf excited plasma. The ion energy and density were such that $5\frac{1}{2}$ hr of bombardment correspond to approximately 10^4 yr of solar-wind action. The normal albedos of the various greenstone surfaces, both before and after bombardment, are given in Table I. These albedo values are plotted vs wavelength in Fig. 1. Also indicated is the region of average lunar values. The albedos of the three larger particle size fractions are very similar to each other before bombardment and also after the 10^4 equivalent year bombardment. All of the particle size fractions would have albedo-wavelength

Table I

Normal Albedos of Sifted Mineral Powders

Material	Size (μ)	Original Powder			10^4 Equiv. Yr			10^5 Equiv. Yr		
		~3700 Å	~5200 Å	~6100 Å	~3700 Å	~5200 Å	~6100 Å	~3700 Å	~5200 Å	~6100 Å
Greenstone	0-20	0.182	0.29	0.305	0.068	0.110	0.130	0.029	0.049	0.062
"	20-44	0.120	0.182	0.187	0.062	0.100	0.115	0.040	0.063	0.073
"	44-74	0.120	0.180	0.180	0.053	0.084	0.092	(0.044	0.063	0.072)*
"	74-300	0.140	0.180	0.170	0.060	0.084	0.091			
Tektite	0-20	0.345	0.420	0.445	0.067	0.130	0.175	0.025	0.053	0.072
"	20-44	0.220	0.340	0.363	0.042	0.103	0.140	0.025	0.048	0.067
"	44-74	0.190	0.305	0.332	0.047	0.110	0.140	(0.030	0.070	0.098)*
"	74-300	0.140	0.252	0.280	0.036	0.095	0.120	(0.019	0.053	0.077)*
Lunar Surface (average)		~0.07	~0.11	~0.14						

* 5×10^4 Equiv. Yr

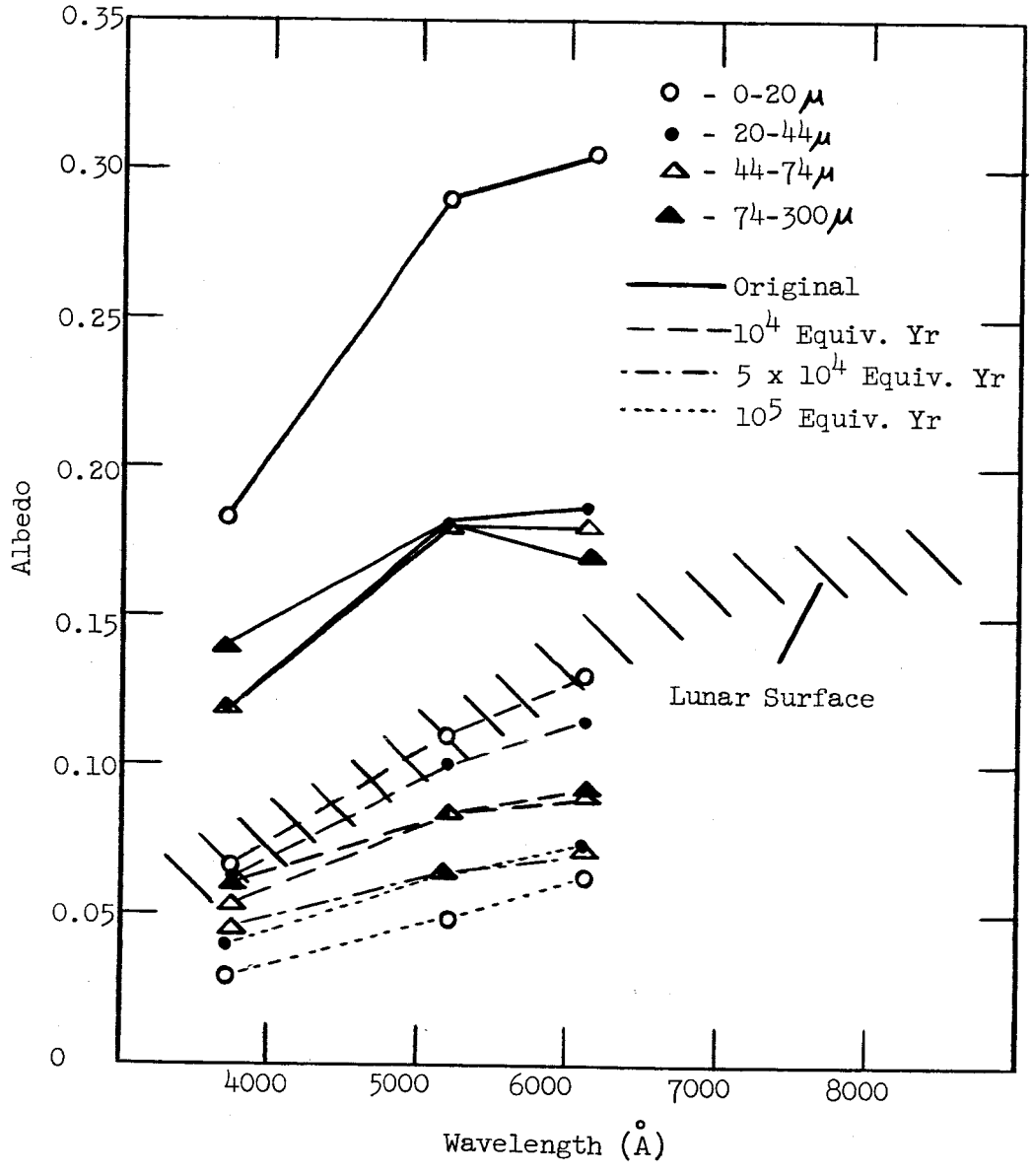

Fig. 1 Albedo vs wavelength for sifted greenstone. Original surface, after the equivalent of 10^4 yr and 5×10^4 or 10^5 yr solar-wind bombardment.

characteristics similar to the average lunar surface in the wavelength region employed after bombardment times equivalent to 10^4 yr solar-wind action or less. Note that further bombardment reduces the albedos to values lower than those for the lunar surface. This illustrates the requirement for a mixing mechanism on the lunar surface. Solar-wind bombardment, as simulated in these studies, would darken every rock powder we have studied to albedos much below the average lunar values in 10^9 yr.

The light reflection curves for greenstone are given in Figs. 2-4. The 0-20 μ particle size surface has the most pronounced optical backscatter and this is enhanced by bombardment. The similarity between the optical reflection characteristics of a bombarded 0-20μ particle greenstone surface and the lunar surface increases with bombardment time. The duration of bombardment necessary for good albedo vs wavelength fit is the equivalent of the order of 10^4 yr while reflection characteristics fit better after the equivalent of the order of 10^5 yr or more. Possibly a bleaching by ultraviolet light could decrease the darkening such that both the albedo-wavelength dependence and the optical scattering properties would be similar to the lunar surface after a given bombardment time.

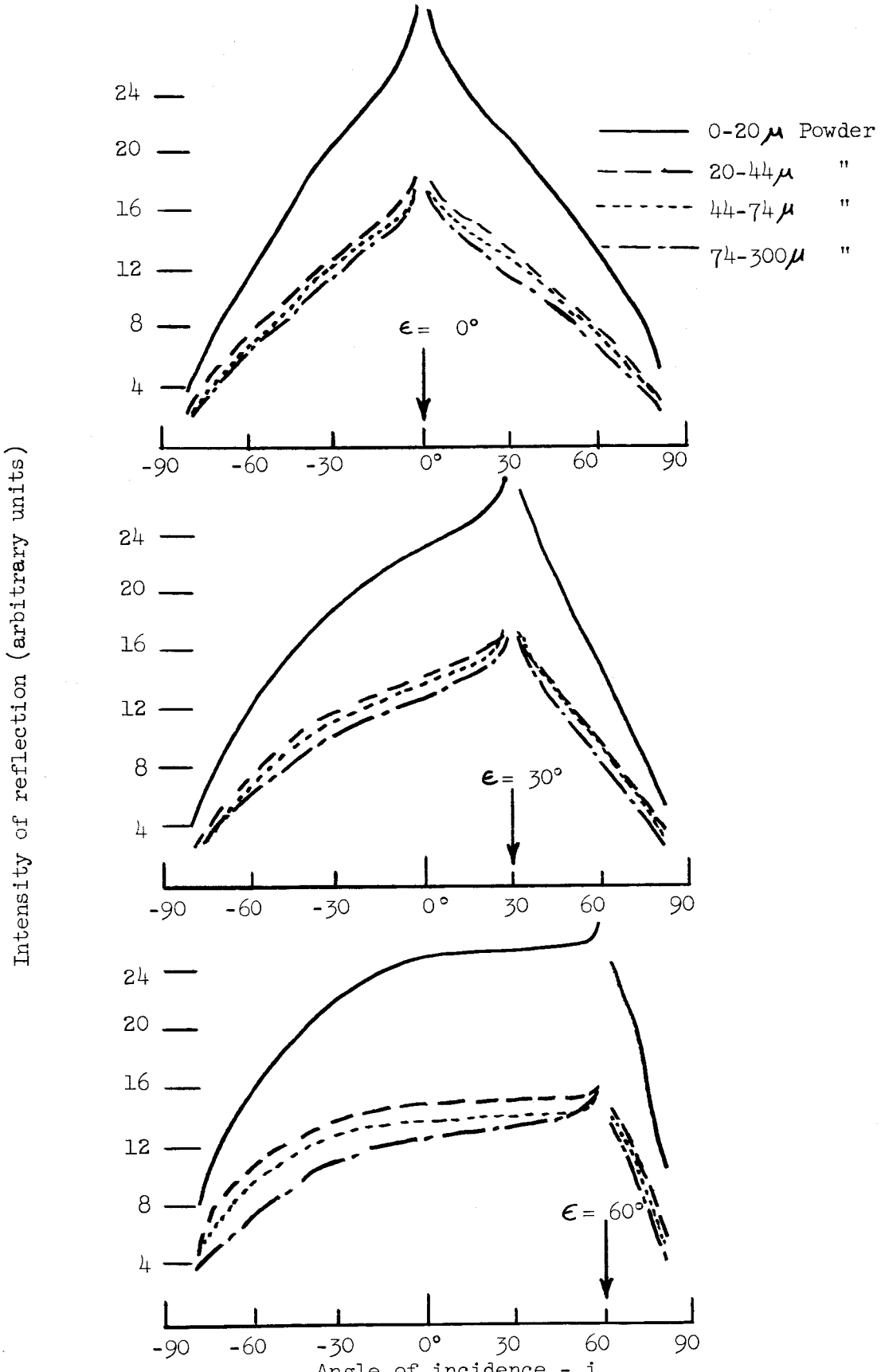

Fig. 2 Reflection curves in green light (~5200 Å) for sifted greenstone of four particle size fractions before bombardment.

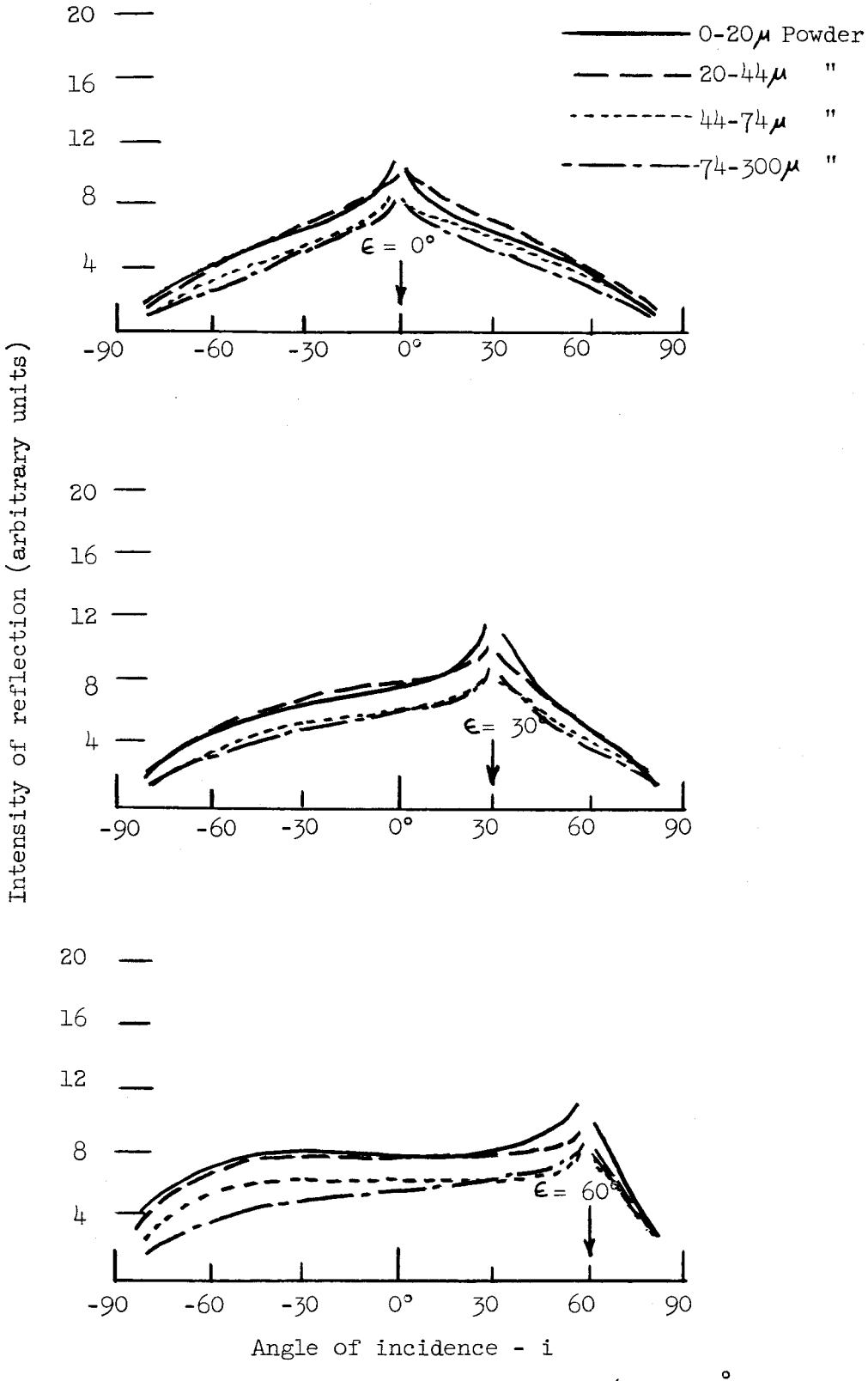

Fig. 3 Reflection curves in green light (~5200 Å for sifted greenstone of four particle size fractions after the equivalent of 10^4 yr solar-wind bombardment.

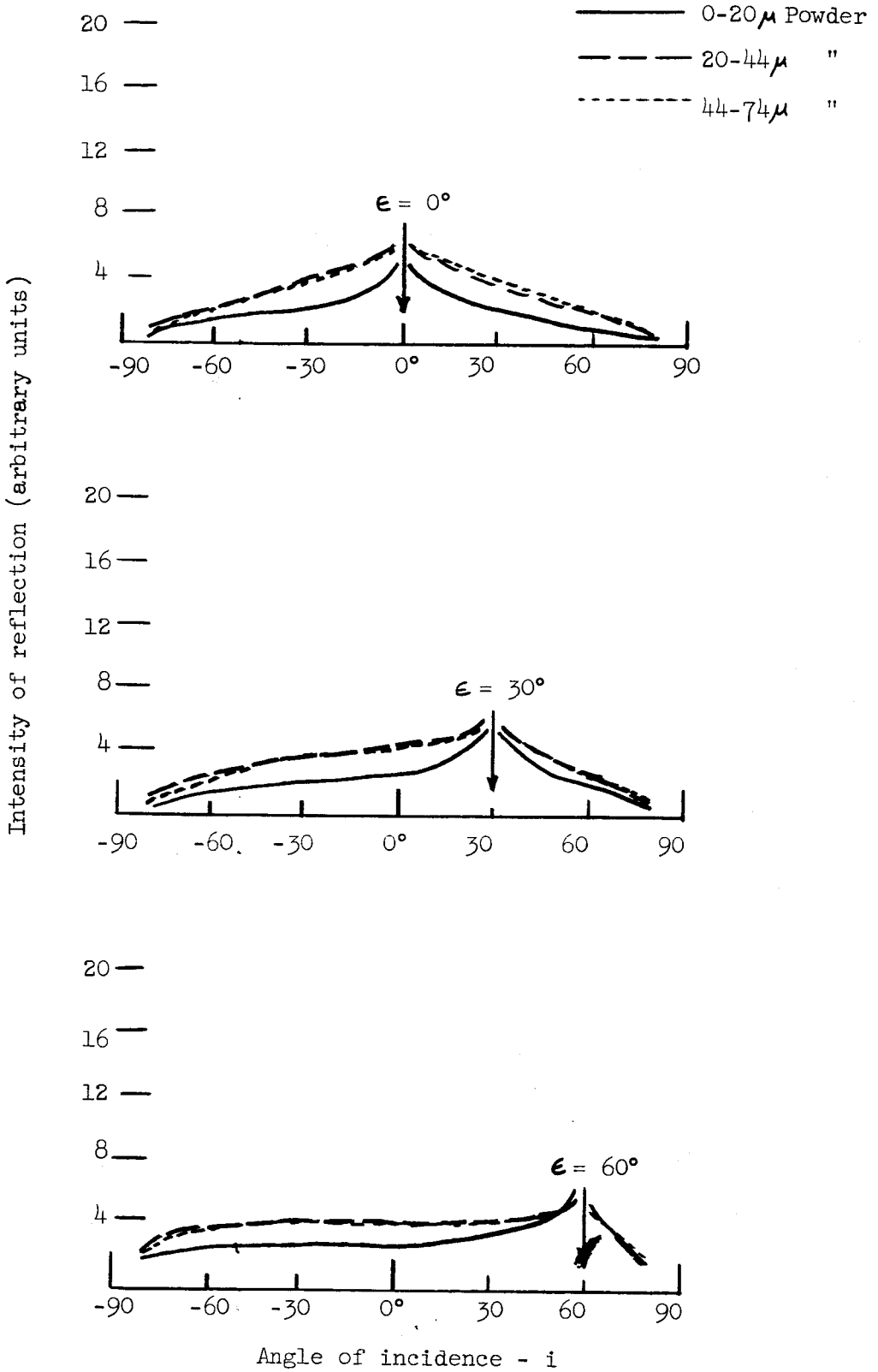

Fig. 4 Reflection curves in green light (~5200 Å) for sifted greenstone of three particle size fractions after the equivalent of 10^5 yr (44-74μ - 5 x 10^4 yr) solar-wind bombardment.

B. Tektite Material

Surfaces of sifted tektite material have been studied in the same manner as surfaces of greenstone. The normal albedos of the surfaces, both before and after bombardment, are given in Table I. The albedos vs wavelength are given in Fig. 5. The region of average lunar values is indicated by the hatched band. For the umbombarded powders the albedo increases with decreasing particle size. After the equivalent of 10^4 yr solar-wind bombardment, the albedos for all four particle size ranges are similar to the lunar average. The increase of albedo with wavelength is a little more pronounced than that of the lunar surface; i.e., the surface is "redder" than the average lunar surface. As with greenstone, additional bombardment continues the darkening. The increase of albedo with wavelength is larger for tektite material than for greenstone even after the equivalent of 10^5 yr of bombardment. Our bombarded materials which are high in silica tend to be "reddish" like the lunar highlands while the more basic materials are more "grey" like the lunar lowlands. The reflection curves for tektite material are given in Figs. 6-8. The 0-20μ particle size surface has a greater degree of optical backscatter than the larger fraction surfaces, but the surface reflection is quite diffuse with appreciable forward scatter even after the equivalent of 10^5 yr of solar-wind bombardment.

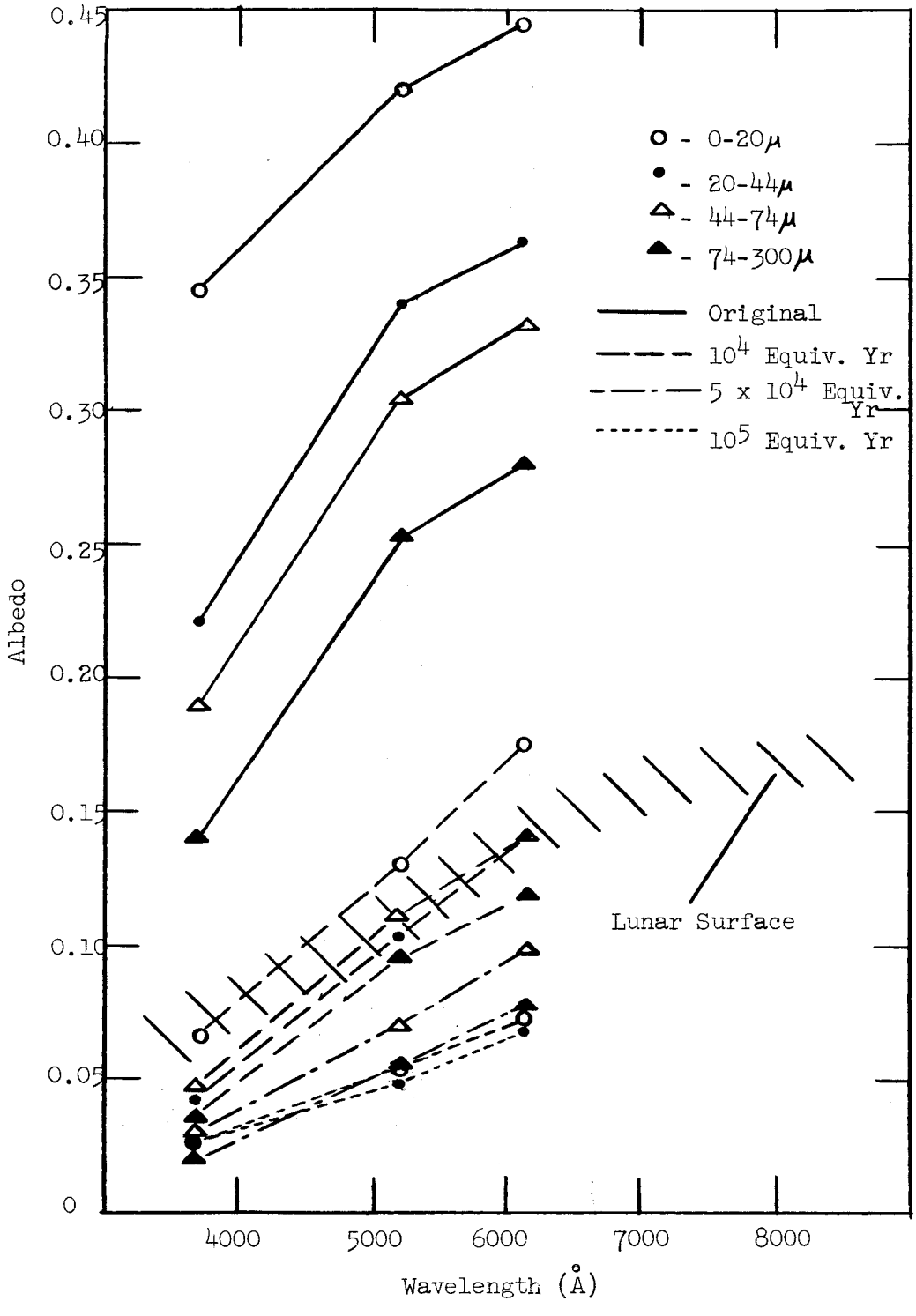

Fig. 5 Normal albedo vs wavelength for sifted tektite material. Original surface, after the equivalent of 10^4 yr and 5×10^4 or 10^5 yr solar-wind bombardment.

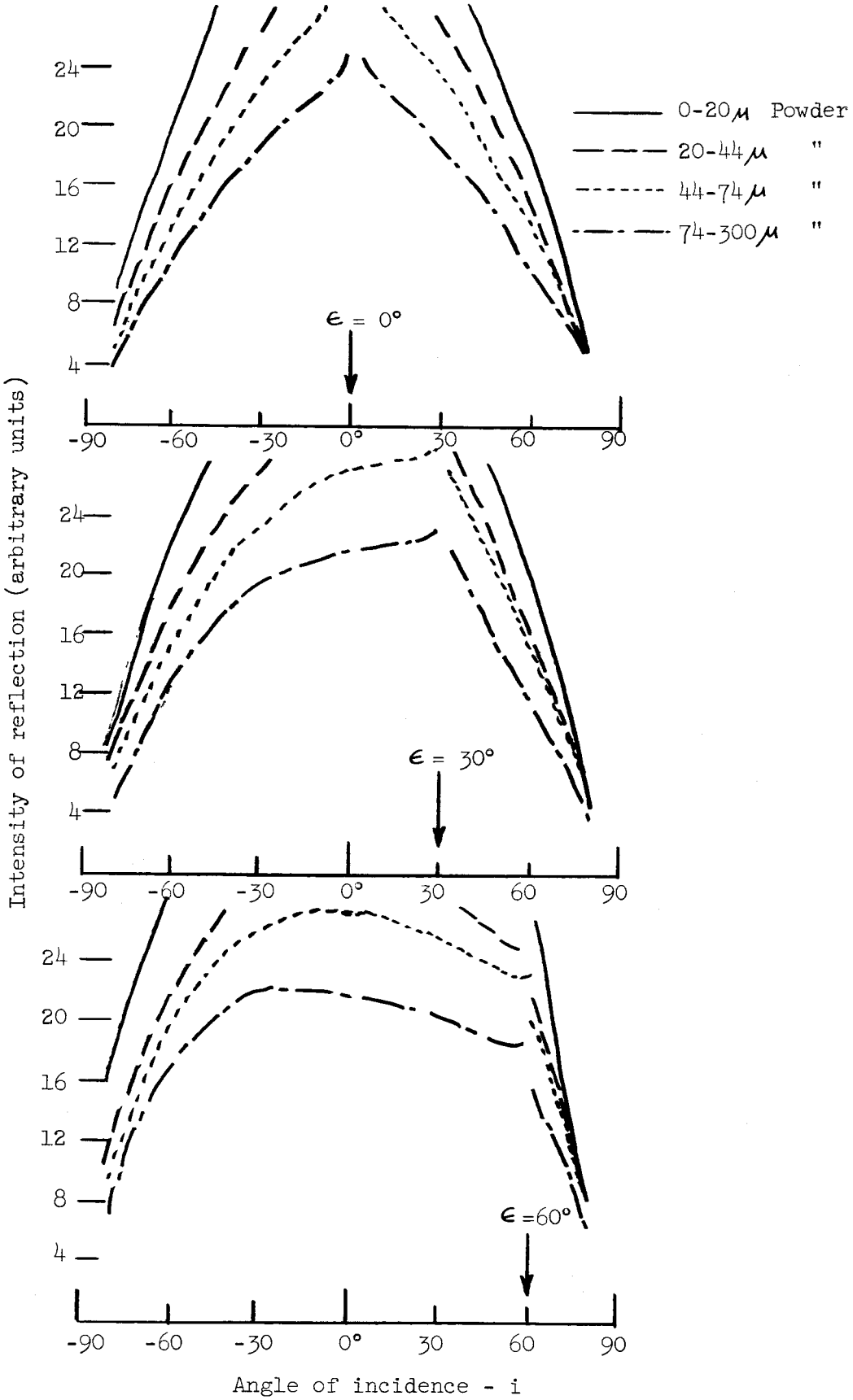

Fig. 6 Reflection curves in green light (~5200 Å) for sifted tektite material of four particle size fractions before bombardment.

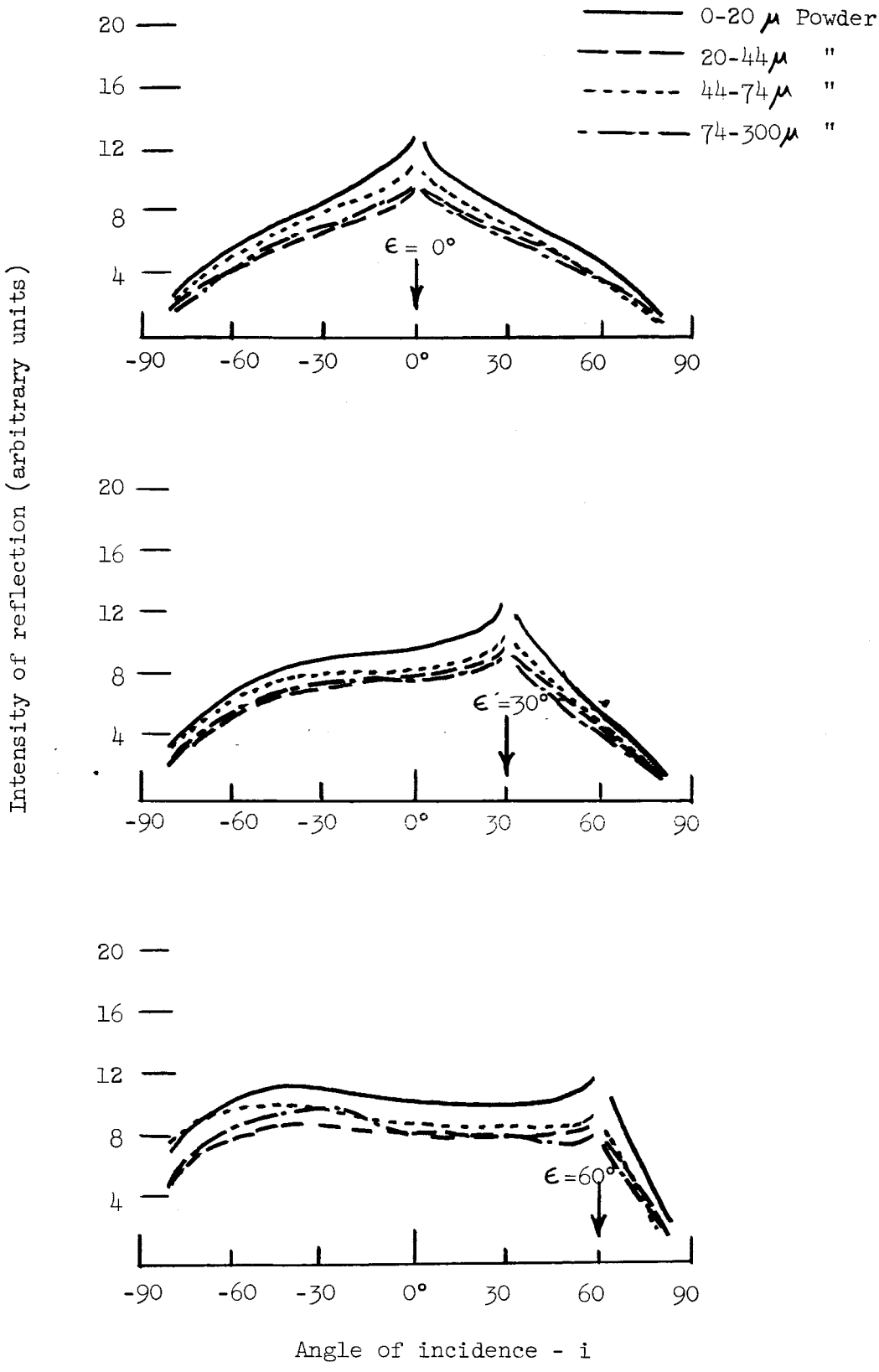

Fig. 7 Reflection curves in green light (~5200 Å) for sifted tektite material of four particle size fractions after the equivalent of 10^4 yr of solar-wind bombardment.

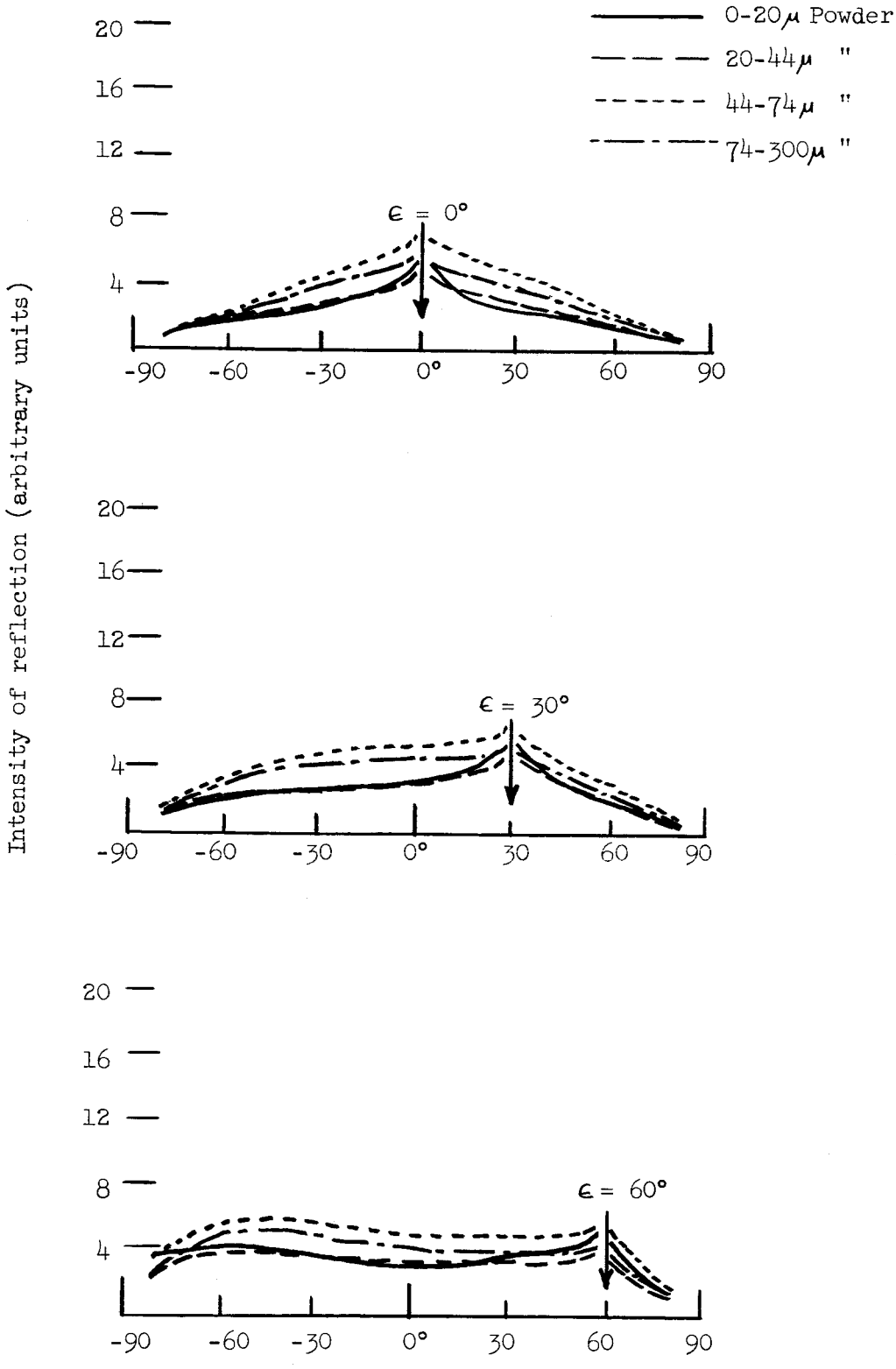

Fig. 8 Reflection curves in green light (~5200 Å) for sifted tektite material of four particle size fractions after the equivalent of 5×10^4 yr (44-74μ and 74-300μ) or 10^5 yr (0-20μ and 20-44μ) solar-wind bombardment.

III. POLARIZATION MEASUREMENTS

The degree of polarization has been measured for green light scattered from greenstone and tektite powders of four size ranges. The results are presented in Figs. 9-16. These measurements extend the program of the previous quarter[1] to additional materials. Analysis of the effect of particle size was previously made for powders of tholeiitic basalt and granodiorite. The additional data strengthen the previous finding that polarization data can be combined with albedos of lunar features to find the size of the particles at the surface of the moon. The effect of composition seems to be confined to its effect on the opacity of the particles of a given size.

Instrumental Effects

We have noticed an asymmetry in the curves obtained for the angle of emergence $\epsilon = 0°$ which seems to be instrumental rather than the consequence of "tilts" of the surface involving dimensions comparable to the 3 mm viewed by the detector. We here indicate evidence that the data for the $\epsilon = 60°$ curves in Figs. 9-16 are not seriously affected by this instrumental difficulty.

Notice that a maximum exists in most $\epsilon = 0°$ curves at a positive phase angle (in our convention) of 70-80° but that no such maximum exists for negative phase angles up to 85°. It is usually the case for fine powders (and apparently for the whole lunar surface) that the degree of polarization is a function only of phase angle in the plane containing the normal to the surface. This means that in general there are two different angles of incidence which give the same degree of polarization for a given angle of emergence.

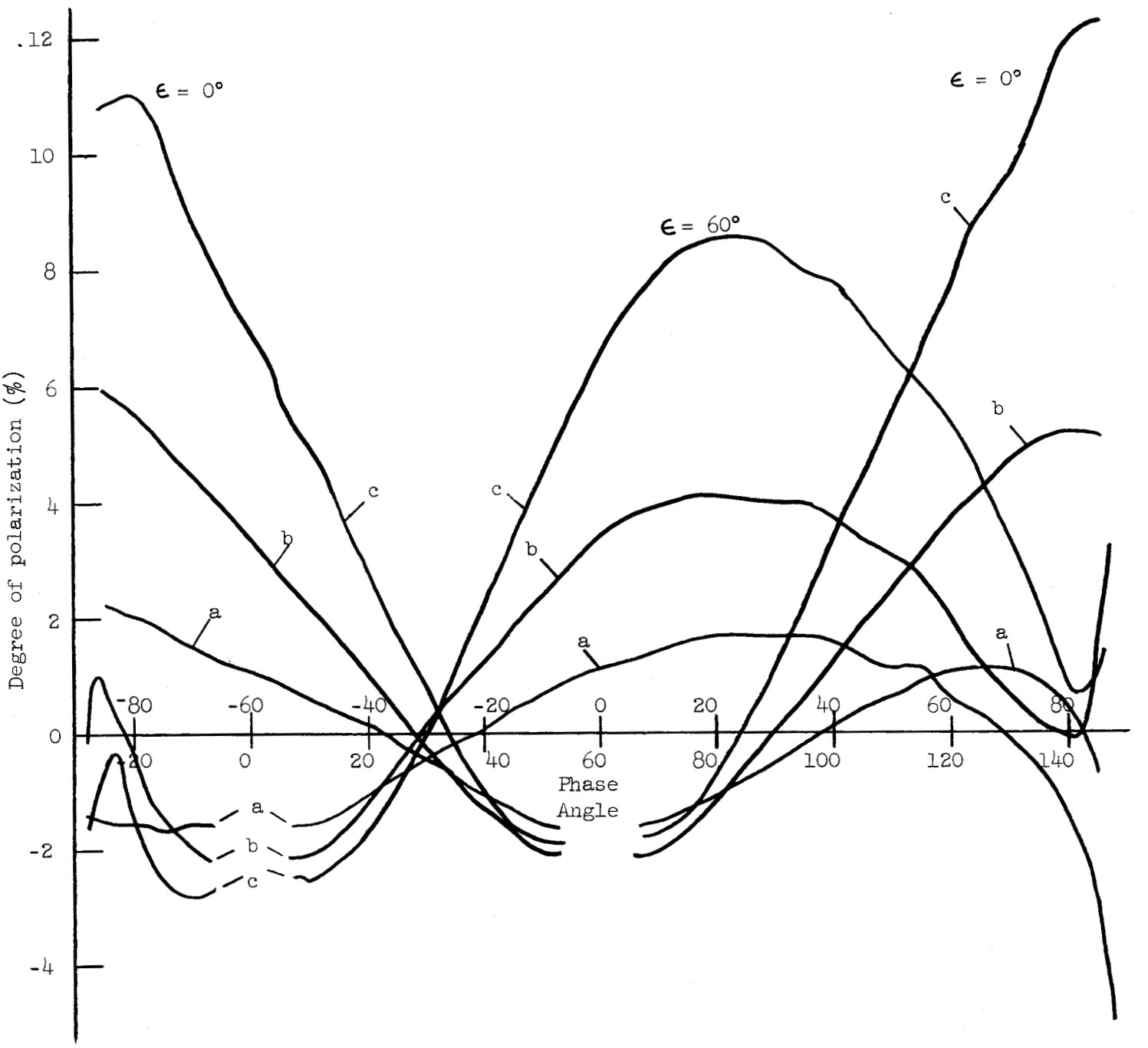

Fig. 9 Polarization of green light scattered from greenstone powder, 0-20μ, sift-74. (a) Unsputtered, $A_n = 0.29$. (b) 10^4 equiv. yr, $A_n = 0.110$. (c) 10^5 equiv. yr, $A_n = 0.049$. The upper and lower abscissa scales refer to $\epsilon = 0°$ and $\epsilon = 60°$, respectively.

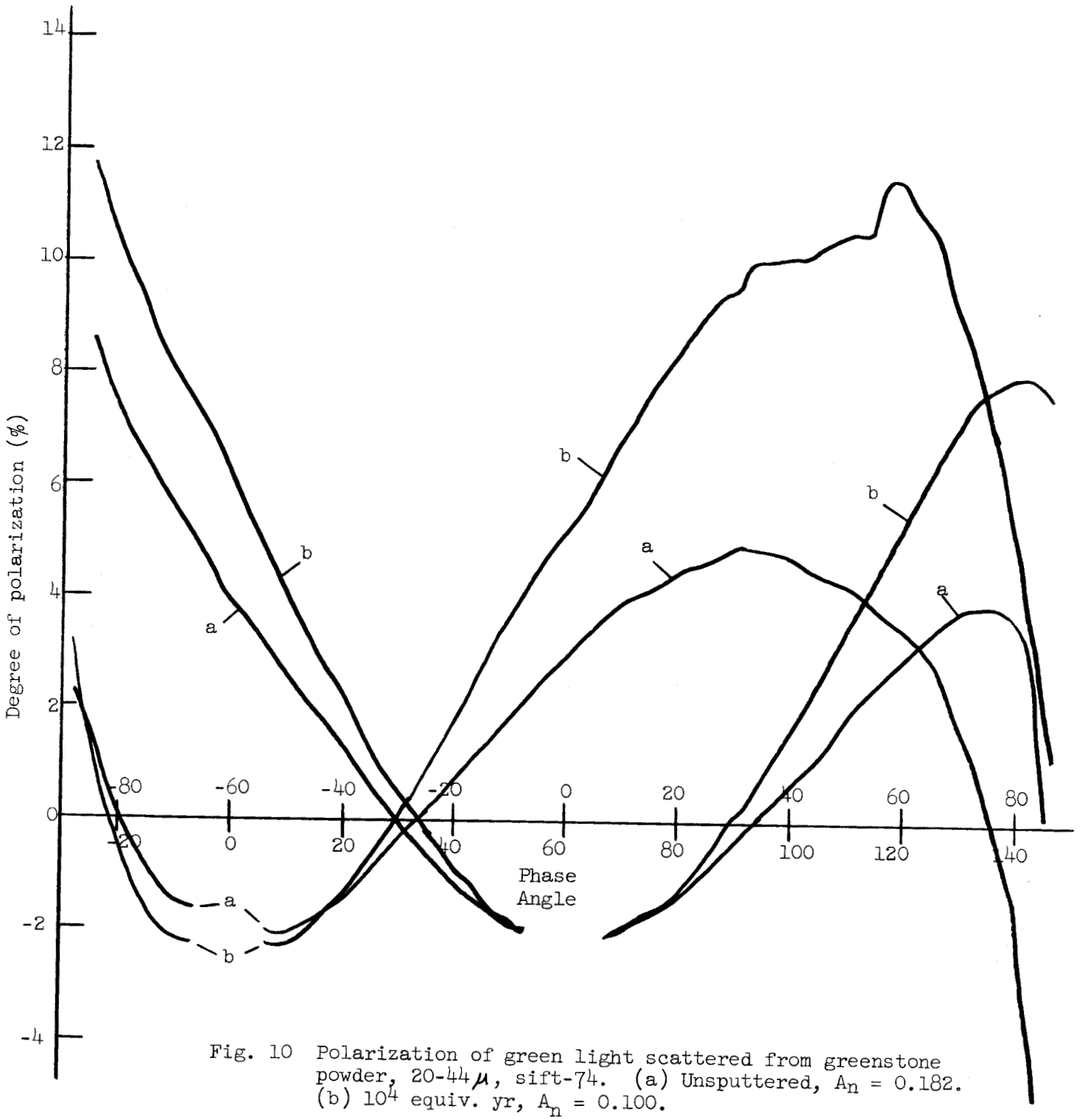

Fig. 10 Polarization of green light scattered from greenstone powder, 20-44μ, sift-74. (a) Unsputtered, A_n = 0.182. (b) 10^4 equiv. yr, A_n = 0.100.

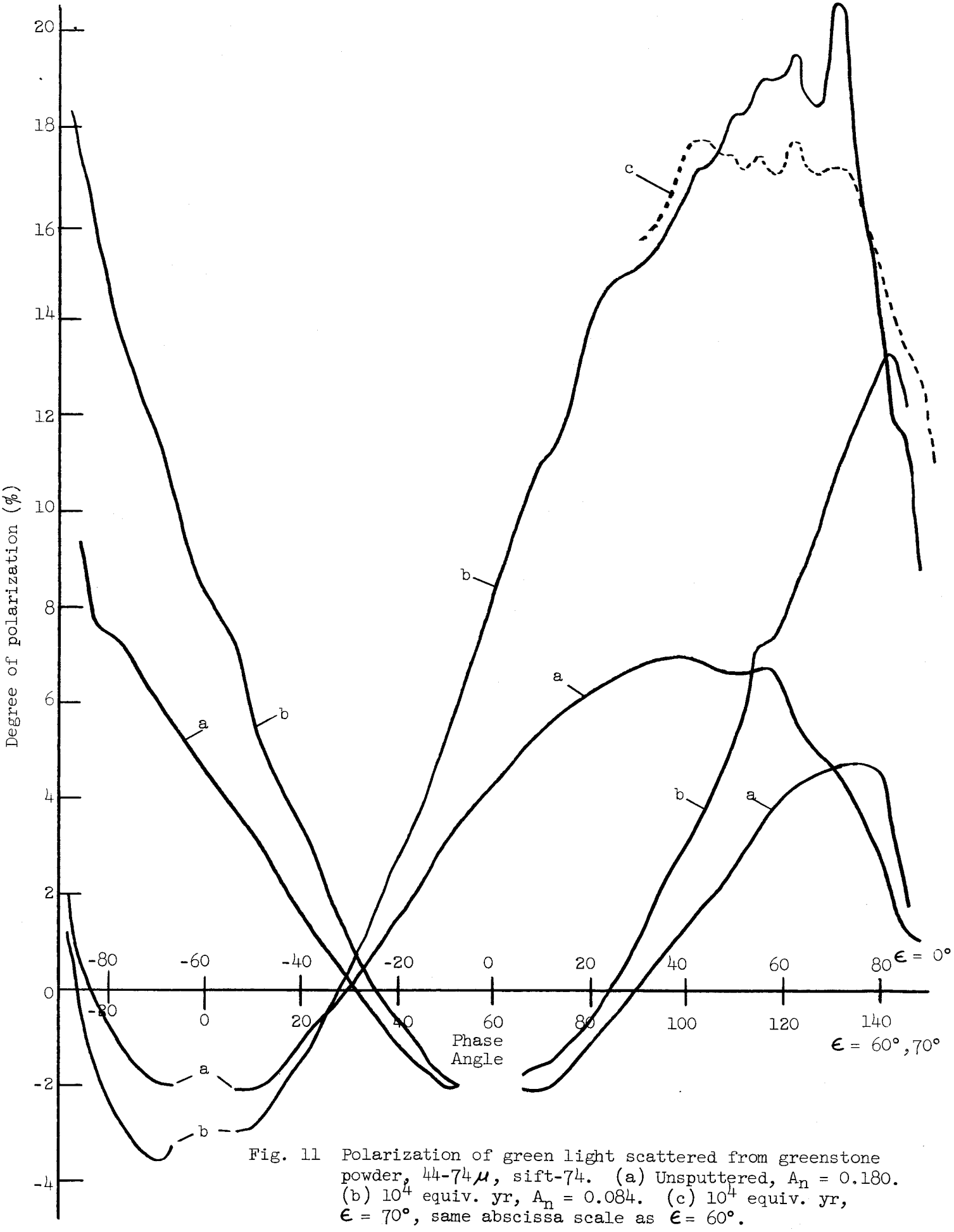

Fig. 11 Polarization of green light scattered from greenstone powder, 44-74μ, sift-74. (a) Unsputtered, A_n = 0.180. (b) 10^4 equiv. yr, A_n = 0.084. (c) 10^4 equiv. yr, ϵ = 70°, same abscissa scale as ϵ = 60°.

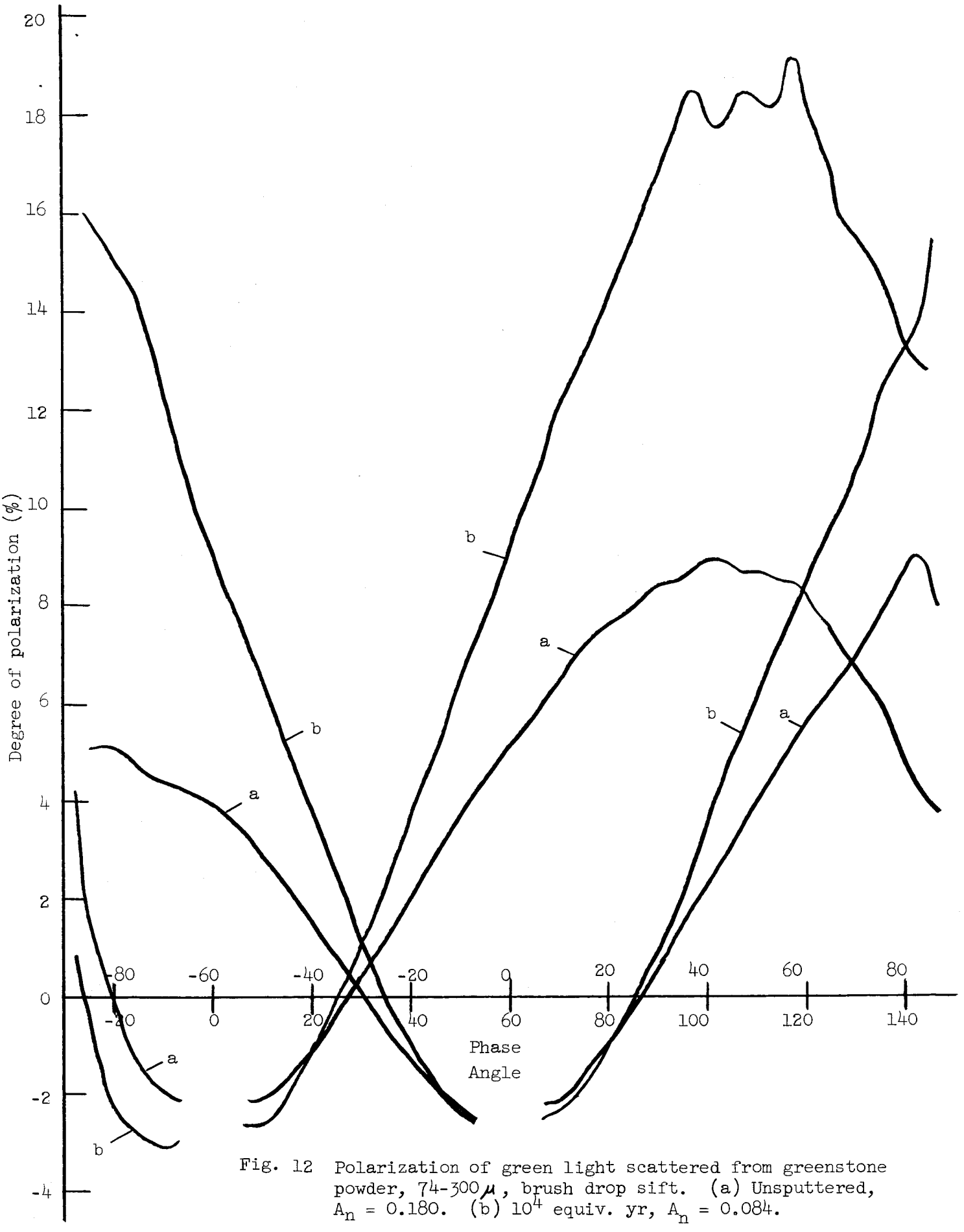

Fig. 12 Polarization of green light scattered from greenstone powder, 74-300μ, brush drop sift. (a) Unsputtered, A_n = 0.180. (b) 10^4 equiv. yr, A_n = 0.084.

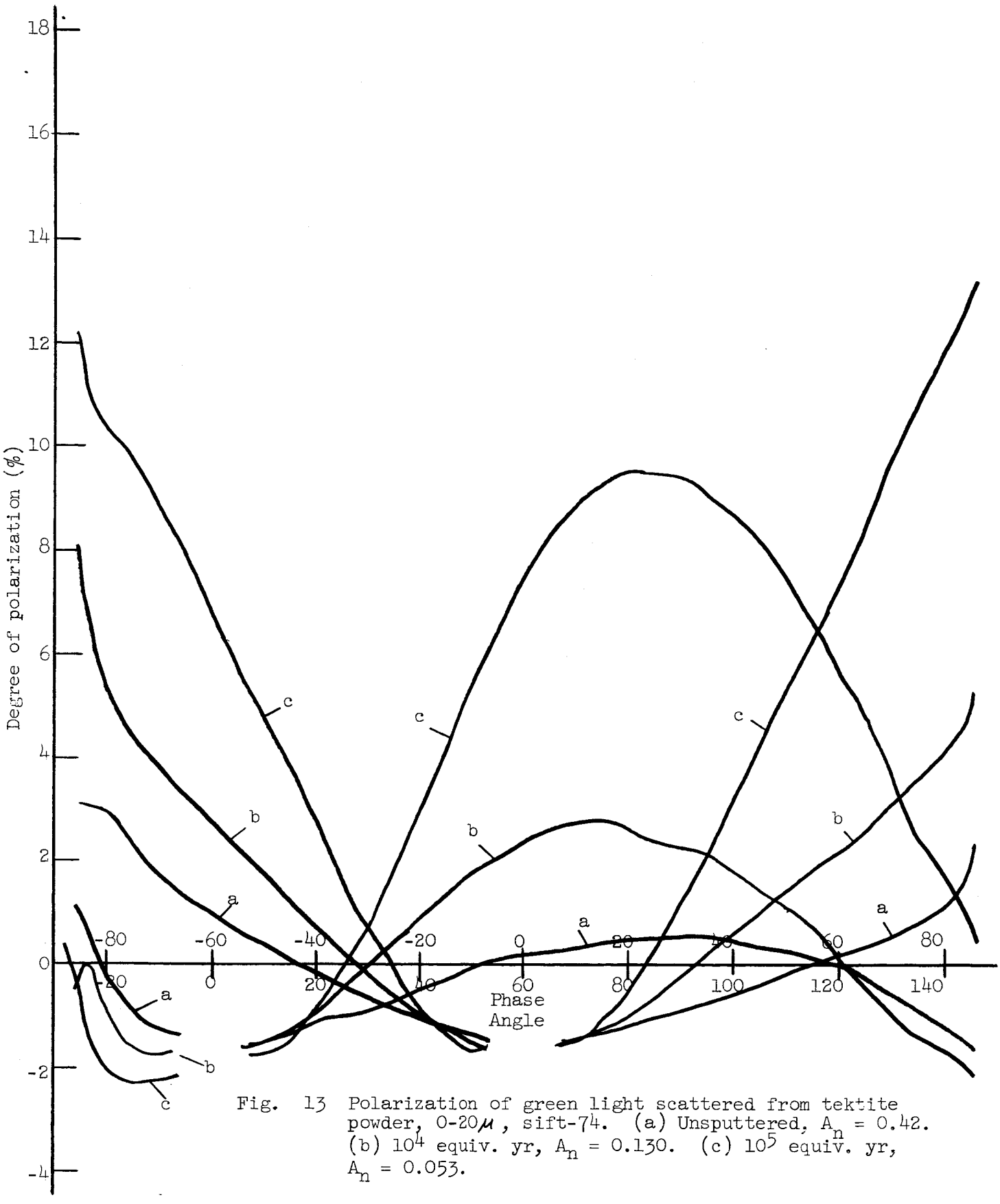

Fig. 13 Polarization of green light scattered from tektite powder, 0-20μ, sift-74. (a) Unsputtered, A_n = 0.42. (b) 10^4 equiv. yr, A_n = 0.130. (c) 10^5 equiv. yr, A_n = 0.053.

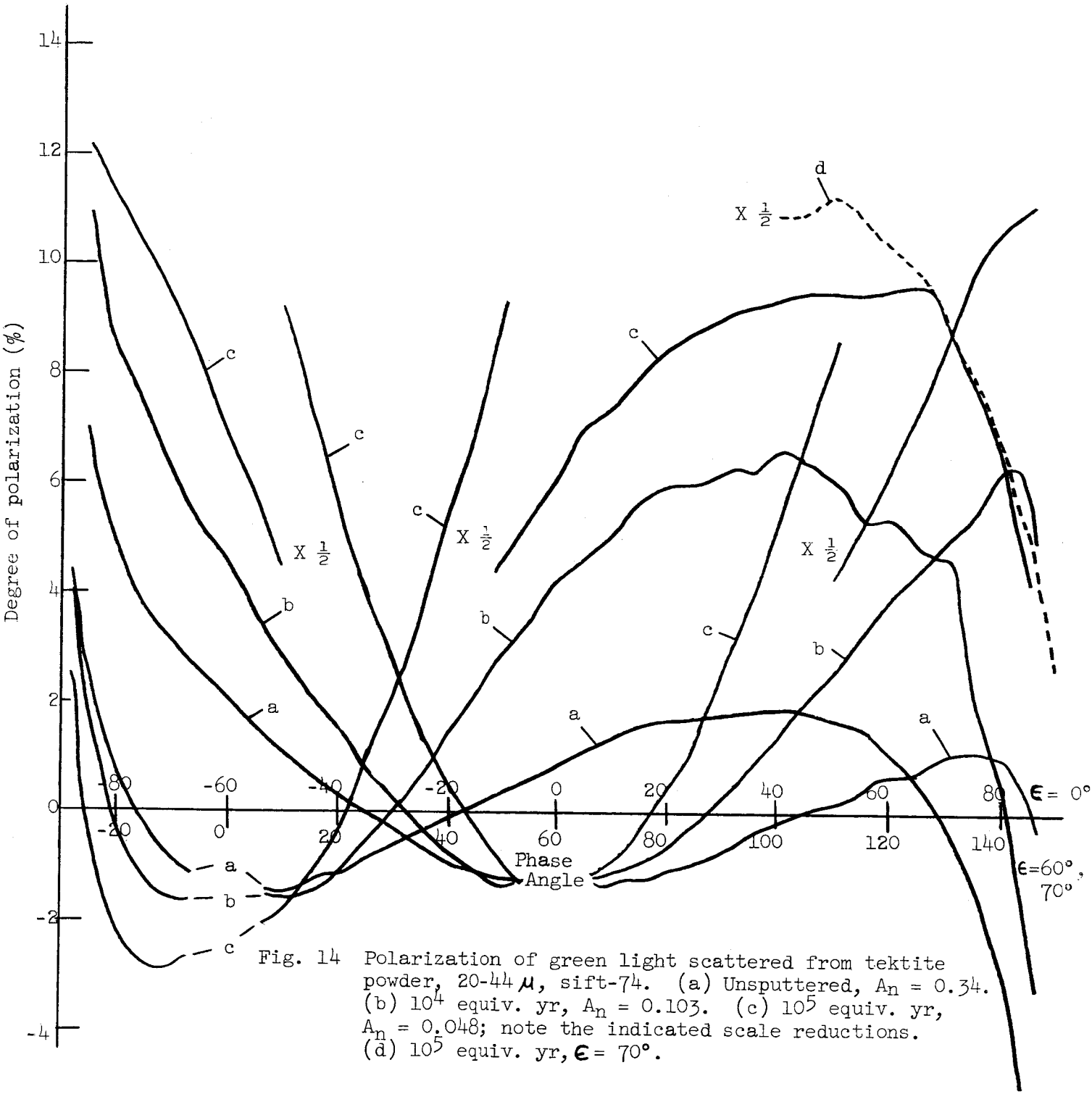

Fig. 14 Polarization of green light scattered from tektite powder, 20-44 μ, sift-74. (a) Unsputtered, A_n = 0.34. (b) 10^4 equiv. yr, A_n = 0.103. (c) 10^5 equiv. yr, A_n = 0.048; note the indicated scale reductions. (d) 10^5 equiv. yr, ϵ = 70°.

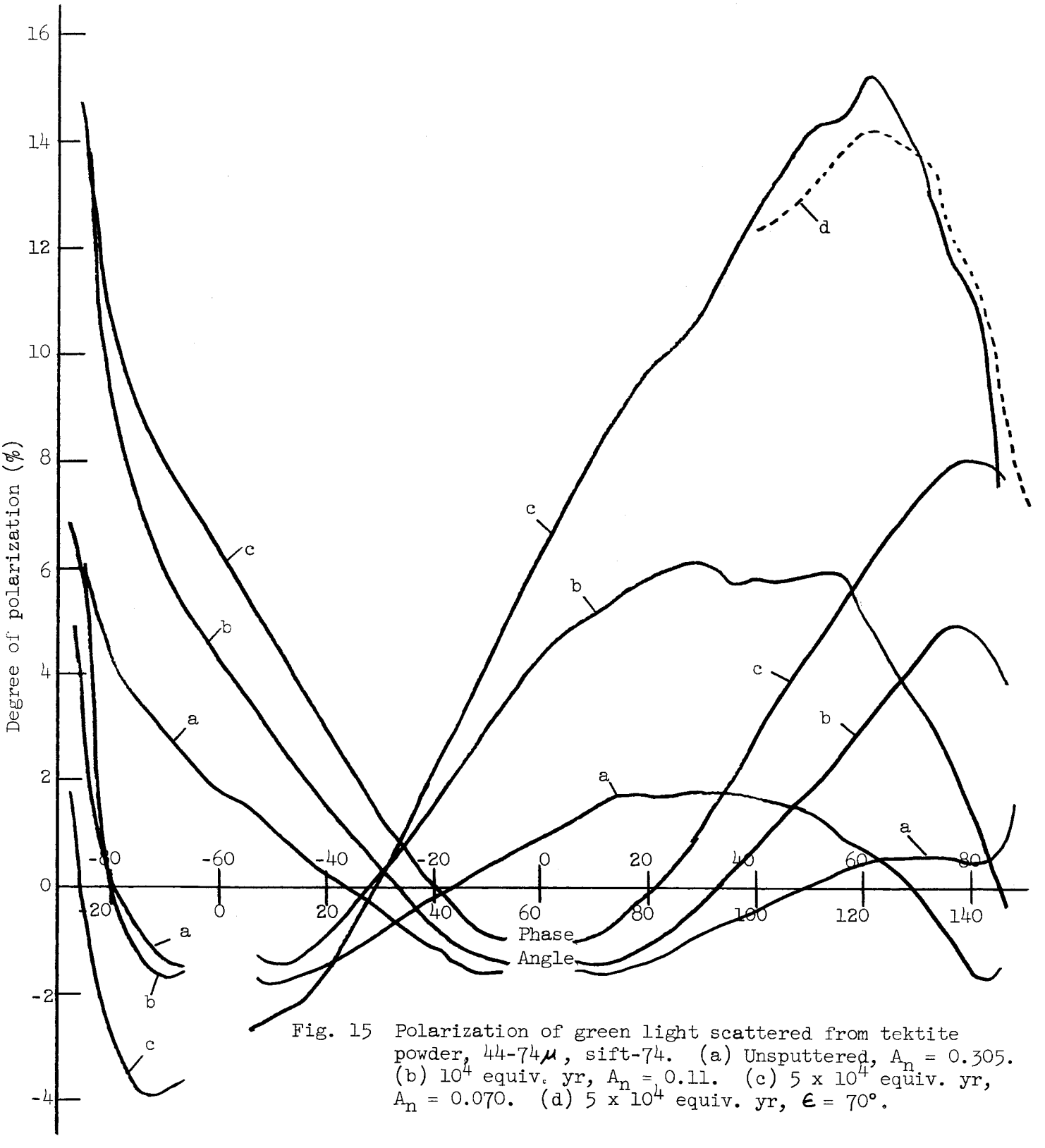

Fig. 15 Polarization of green light scattered from tektite powder, 44-74μ, sift-74. (a) Unsputtered, $A_n = 0.305$. (b) 10^4 equiv. yr, $A_n = 0.11$. (c) 5×10^4 equiv. yr, $A_n = 0.070$. (d) 5×10^4 equiv. yr, $\epsilon = 70°$.

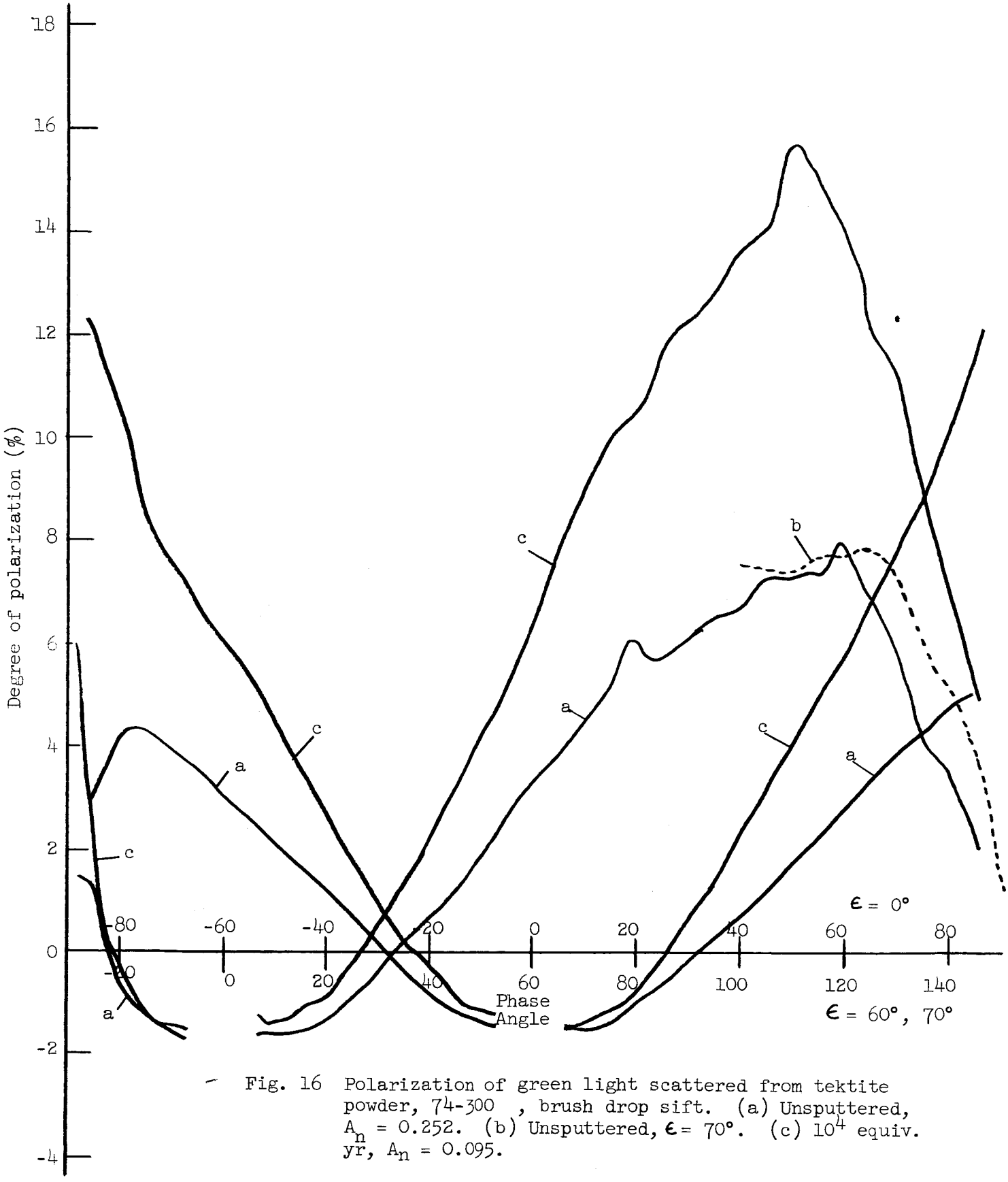

Fig. 16 Polarization of green light scattered from tektite powder, 74-300 , brush drop sift. (a) Unsputtered, A_n = 0.252. (b) Unsputtered, ϵ = 70°. (c) 10^4 equiv. yr, A_n = 0.095.

Viewing at 45° from the surface normal, for example, polarization will be the same for light of near glancing incidence and of near normal incidence. But in our apparatus we presently find systematic deviations from this rule such that for phase angle $|\alpha| = 80°$, the degree of polarization increases in the following order of curves (e.g., Fig. 9): $+\alpha$ for $\epsilon = 0°$, $+\alpha$ for $\epsilon = 60°$, $-\alpha$ for $\epsilon = 0°$. No such systematic changes should be found at different angles of emergence. At a given phase angle in excess of 60°, the curve for the angle of emergence $\epsilon = 60°$ is approximately the geometric mean of the two curves for $\epsilon = 0°$. In addition to the large effects for large phase angles, there may also be a very small systematic asymmetry for the $\epsilon = 0°$ case at small phase angles. All these systematic asymmetries can be attributed to problems with the light source, e.g., a non-uniform illumination by slightly polarized light that approximates uniform illumination by unpolarized light at small phase angles. In the future, attempts will be made to remove the asymmetries associated with the light source by observing light scattered from "simple" surfaces and then realigning the optics. Before this realignment, an instrumental function should be obtained which will permit approximate correction of earlier data, especially those for $\epsilon = 0°$.

The effect of light source asymmetry upon the degree of polarization is small except for glancing incidence and becomes smaller as ion bombardment darkens a given surface. This can be seen, for instance, in Fig. 14 where the two $\epsilon = 0°$ curves are in fair agreement for the unsputtered sample to a phase angle of 40°. As the albedo decreases due to ion bombardment and polarization increases for phase angles in excess of 30°, the asymmetry becomes relatively less important, even at a phase angle as high as 85°.

In some of the figures there is a bombardment-induced asymmetry which is not instrumental. Notice, for instance, that while the two curves for $\epsilon = 0°$ in Fig. 14 converge to a single function of phase angle as the albedo decreases, the two curves for $\epsilon = 0°$ lie higher than the corresponding functions for $\epsilon = 60°$, especially at small phase angles. Notice also that the obvious symmetry about zero phase angle for the $\epsilon = 0°$ case is not shared by the $\epsilon = 60°$ case. Rather, the region of negative degree of polarization becomes more and more marked for the $\epsilon = 60°$ case as bombardment proceeds. These systematic shifts of the polarization curve that cause asymmetry about an oblique viewing angle are not instrumental. In a previous report[3] this phenomenon was attributed to the effects of ion bombardment in a fixed direction normal to the target surface (vertical) and is therefore a property of the powder sample. It was later asserted[1] that a pattern of vertical shadows in the scatterer constitutes a boundary condition that gives rise to enhancement of the polarization (of the electric vector) in the vertical direction.

We presently consider that the asymmetry of the light source has not markedly affected the degree of polarization for the $\epsilon = 60°$ measurements up to phase angle $\alpha = +130°$. In particular, since the phase angle of maximum degree of polarization, α_+, lies generally between 80 and 130°, we believe that the region of maximum degree of polarization has been negligibly affected by the light source asymmetry. The worst asymmetry is for small particles of high albedo, but in that case $\alpha_+ \simeq 80°$ so that for $\epsilon = 60°$, the angle of incidence giving maximum polarization is only 20° beyond the sample normal. The effect of the asymmetry of the light source should be minimal for such near-normal incidence.

In addition to light source difficulties, there is another type of instrumental difficulty that affects the interpretation of the data of Figs. 9-16. In Figs. 12 and 16, for example, but in other curves as well, there are oscillations of the polarization curve in angular intervals of about 5°. Let us refer to this phenomenon as the "facet effect" because, in fact, it is relatively more serious as particle size increases and if specular reflection is marked. In studies of ion-bombarded fracture surfaces of rock,[3] we found that specular reflection at a large phase angle is accompanied by polarization approaching 100% in a small angular interval, even though the surface is quite rough. Consider that a detector of polarization views a sample area of dimension L. It is clear that as the particle size of a powder sample increases toward L, the possibility of detecting a discrete enhancement of polarization in a small angular interval due to a strong beam of light from a few facets increases. If many facets must cooperate to give a detectable effect, then depressions of the polarization as well as enhancements should be equally possible at some other phase angle. If too many facets must cooperate, then it is improbable that any facet effect will be detected. In our apparatus, L = 3 mm = 3000μ. The particles in Figs. 12 and 16 range up to 0.1 L in size and the facet effect is quite bothersome in the region of maximum degree of polarization. The particles of Figs. 9 and 13 are less than 0.07 L and the facet effect is negligible.

Interpretation of the Measurements

It is obvious from Figs. 9-16 that the polarization of light scattered from larger (or darker) particles is markedly greater. Since the polarization evidently depends upon two variables, we can plot some polarization parameter vs normal albedo and treat particle size as a parameter. For basalt and granodiorite powders,[1] we plotted the maximum degree of polarization, P_+. For linear coordinates we found hyperbola-like curves. The results are replotted with logarithmic coordinates in Fig. 17. The points now lie on nearly straight lines. Assumption of a relation $P_+ = kA_n^{-m}$ requires $m \cong 1.3$ where A_n is the normal albedo. The corresponding data for greenstone and tektite powders in Fig. 18 are very similar. All of these data are listed in Table II. The phase angle, α_+, at which P_+ was observed is also listed in Table II. The values of P_+ and α_+ are estimated in terms of a smoothed curve so as to eliminate the facet effect. In cases when α_+ approached 120°, an auxiliary curve for $\epsilon = 70°$ was usually obtained because there was the possibility that specular reflection might enhance the polarization at $\alpha = 120°$ for $\epsilon = 60°$. Except for the largest particle sizes in each rock type, there was no specular enhancement for these sifted powders. The presence of specular enhancement for bombarded powders that were not sifted in preparation has been noted.[3]

In Figs. 17 and 18, the region of corresponding lunar values of P_+ and A_n is indicated by a rectangle. The available lunar values are plotted in Fig. 19, listed in Table III, and discussed further in the Appendix.

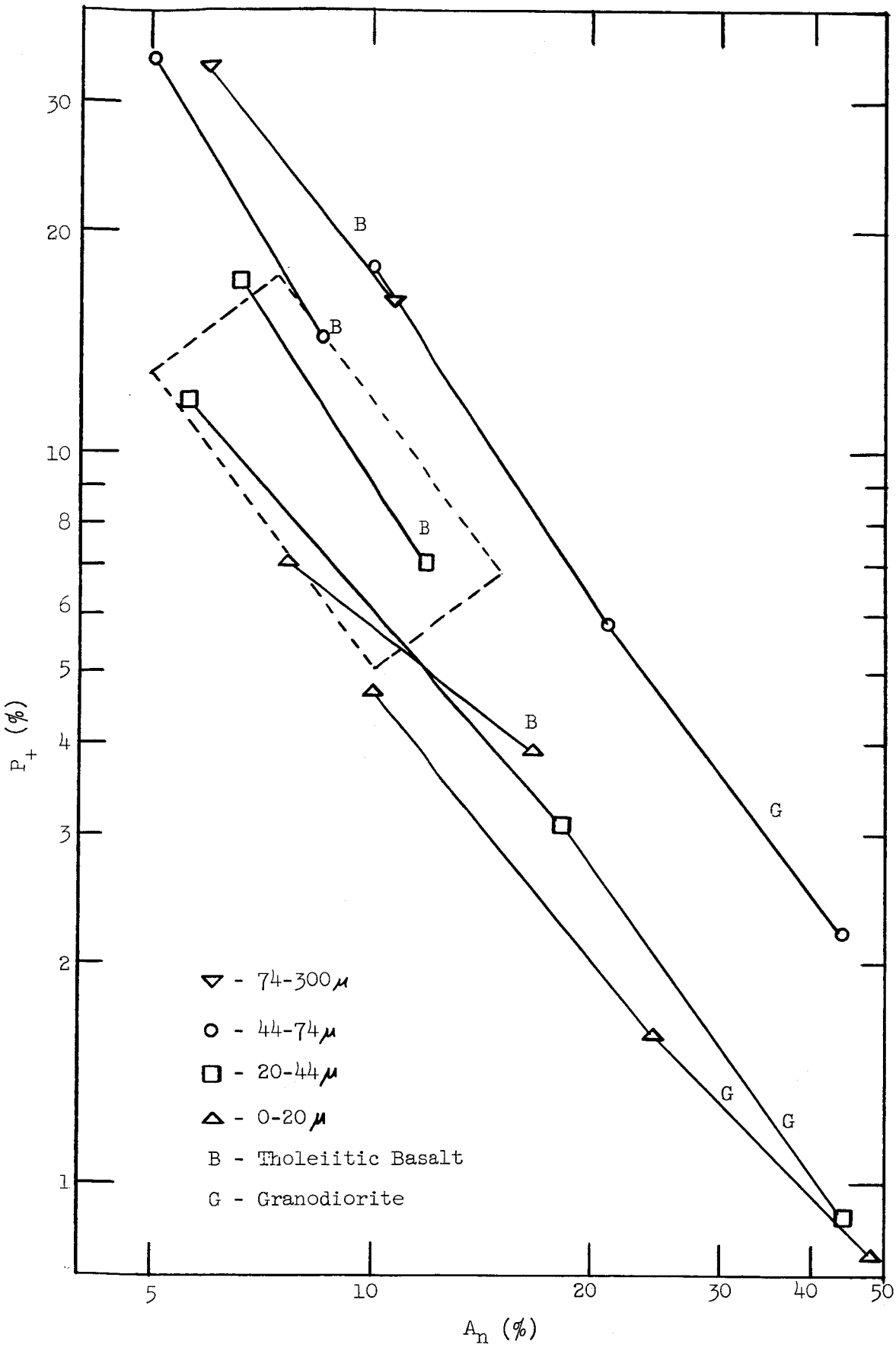

Fig. 17 Maximum polarizations and albedos of tholeiitic basalt and granodiorite powders of graded sizes. The range of lunar values is indicated by the dotted rectangle.

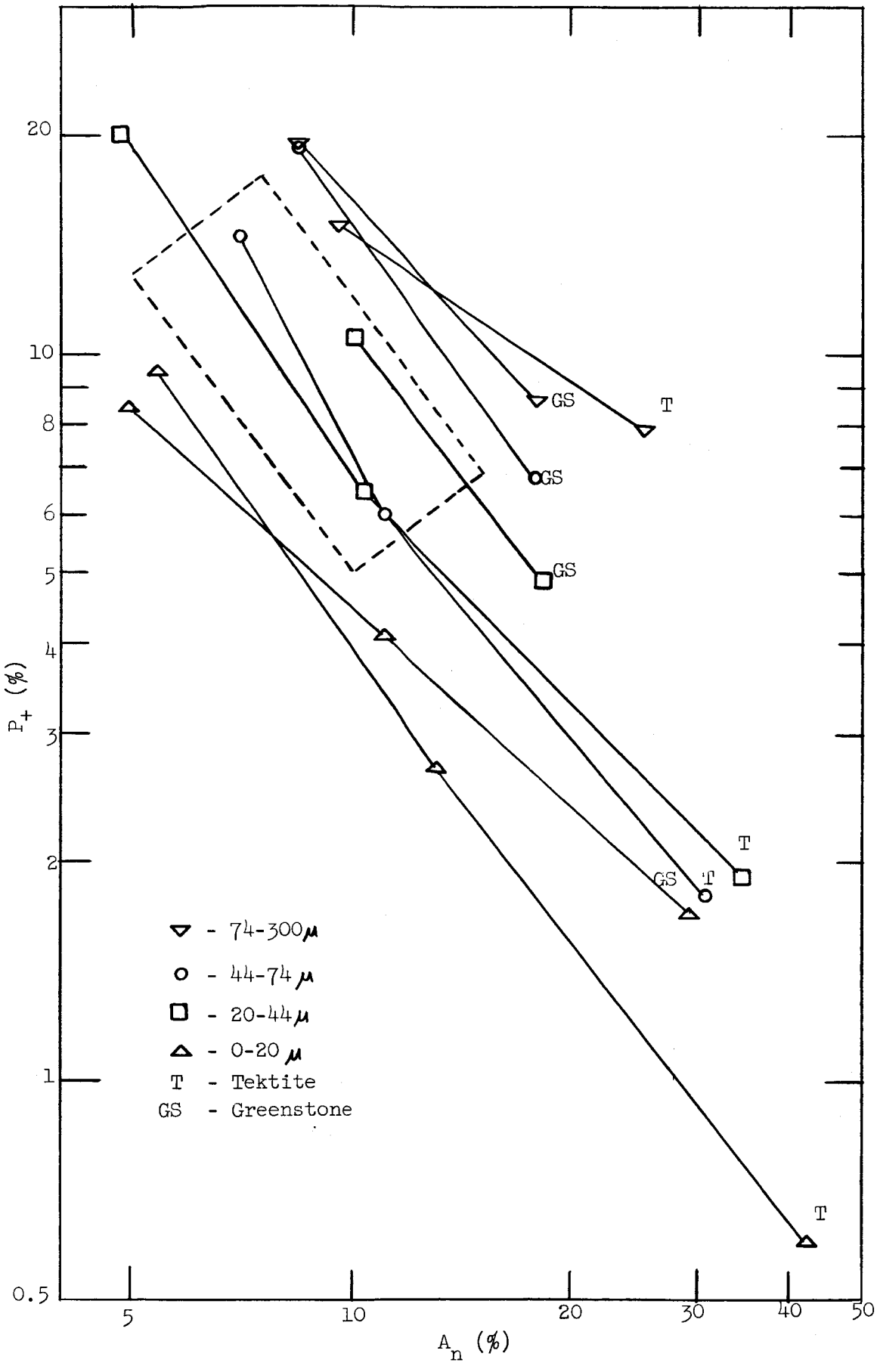

Fig. 18 Maximum polarizations and albedos of greenstone and tektite powders of graded sizes.

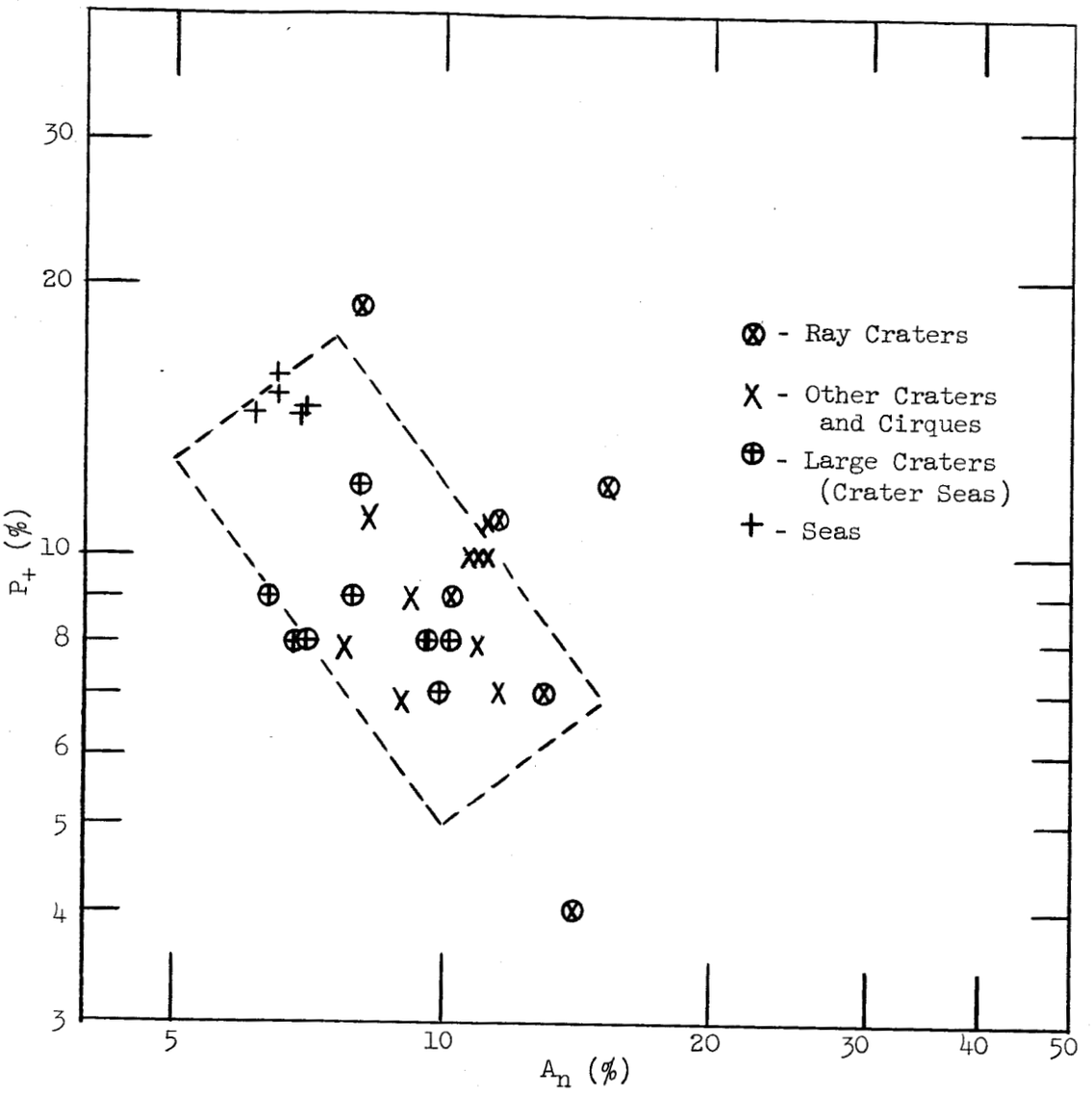

Fig. 19 Maximum polarizations and albedos of lunar features of various geological types.

Table II

Albedo and Polarization Parameters
Measured for Rock Powder Samples

Material	Size (μ)	Log_{10} Age (Equiv. Yr)	A_n (Green)	P_+ (%)	Est. α_+ (Deg)	PR (%)	P_+/PR
Tholeiitic Basalt	0-20	2*	0.167	3.9	82	3.95	0.99
		4	0.077	7.1	88	6.65	1.07
"	20-44	2	0.118	7.1	91	6.2	1.15
		4	0.066	17.1	106	10.35	1.65
"	44-74	2	0.085	14.4	100	10.7	1.35
		4	0.050	34.4	112	16.9	2.04
"	74-300	2	0.107	16.1	97	10.7	1.50
		4	0.059	33.6	116	16.0	2.10
Granodiorite	0-20	2	0.48	0.8	90:	1.25	0.64
		4	0.242	1.6	80	2.0	0.80
		5	0.10	4.7	83	4.5	1.04
"	20-44	2	0.443	0.9	92	1.6	0.56
		4	0.182	3.1	84	3.1	1.00
		5	0.056	11.8	85	8.2	1.44
"	44-74	2	0.44	2.2	90:	1.95	1.13
		4	0.210	5.8	102	3.5	1.66
		5	0.100	18:	130:	5.8	3.10
Greenstone	0-20	2	0.29	1.7	90	2.2	0.77
		4	0.110	4.1	78	4.6	0.89
		5	0.049	8.5	85	8.25	1.03

Table II (Cont'd.)

Material	Size (μ)	Log_{10} Age (Equiv. Yr)	A_n (Green)	P_+ (%)	Est. α_+ (Deg)	PR (%)	P_+/PR
Greenstone	20-44	2*	0.182	4.9	91	4.4	1.11
		4	0.100	10.6	110:	6.65	1.59
"	44-74	2	0.180	6.8	98	5.4	1.26
		4	0.084	19.2	120	9.8	1.96
"	74-300	2	0.180	8.7	102	6.2	1.40
		4	0.084	19.5:	108:	10.2	1.91
Tektite	0-20	2	0.42	0.6	90	1.3	0.46
		4	0.130	2.7	77	3.35	0.81
		5	0.053	9.5	83	8.4	1.13
"	20-44	2	0.34	1.9	100:	3.05	0.62
		4	0.103	6.5	95	5.3	1.23
		5	0.048	20	115:	12.8	1.56
"	44-74	2	0.305	1.8	90	2.4	0.75
		4	0.11	6.1	95	5.3	1.15
		4.7	0.070	14.5	120	7.85	1.85
"	74-300	2	0.252	7.8	121	4.6	1.69
		4	0.095	15	113	7.2	2.08

*Unsputtered samples are indicated by an age whose logarithm is given as 2 for convenience.

Values that are particularly uncertain are indicated by a colon (:).

Table III

Polarization Characteristics of Lunar Features with Corresponding Albedos

No.	Name	P_+ (a)	P_+ (Ref.10)	A (b)	A (Ref.4)	A (Ref.11)
	MARIA					
1	Sinus Iridum	16 ± 1	12.6	0.07		0.065
2	Mare Crisium, center	14.5 ± 1		0.09		
	" " , south	13 ± 1		0.10		
	" " , north		14.7			
3	Mare Nectaris, center	13.5 ± 0.5				
	" " , south	12.5 ± 0.5		0.11		
4	Mare Foecunditatis, east of Messier	15 ± 1				0.069
	" " , west of Messier		14.0			
5	Mare Serenitatis		14.7 (Ref.13)			0.070
6	Mare Tranquilitatis		15.2 (Ref.13)			0.066
	THE BOTTOM OF CRATERS AND CIRQUES					
7	Albategnius	11 ± 1			0.111	0.112
8	Alphonsus	10 ± 1		0.13	0.107	
9	Artistarchus (ray crater)	12.0 ± 1.4		0.26	0.152	0.176
10	Artistillus (ray crater)	19 ± 1			0.080	
11	Aristoteles	9 ± 1			0.105	0.110
12	Arzachel	10 ± 1		0.13	0.112	
13	Autolycus	11		0.10	0.082	

Table III (Cont'd.)

No.	Name	P_+ (a)	P_+ (Ref.10)	A (b)	A (Ref.4)	A (Ref.11)
14	Catharina	7		0.15	0.115	
15	Cleomedes		6.8 (Ref.13)		0.090	
16	Copernicus (ray crater)	11		0.13	0.114	0.120
17	Cyrillus	10		0.15	0.110	
18	Gassendi	9 ± 1		0.11	0.091	
19	Kepler (ray crater)	9		0.13	0.102	0.100
20	Picard		9.4 (Ref.13)			
21	Posidonius	8		0.09	0.077	
22	Proclus (ray crater)	4		0.21	0.142	
23	Theophilus	8		0.15	0.108	
24	Tycho (ray crater)	7		0.18	0.131	0.154
	CRATER "SEAS"					
25	Archimedes	12		0.10	0.081	0.088
26	Fracastorius	8		0.14	0.102	
27	Grimaldi, north	9		0.05	0.063	0.062
	" , south	9		0.07		
28	Plato	8		0.07	0.068	0.068
29	Plotemaus	8		0.11	0.095	0.108
30	Riccioli	8			0.071	0.060
31	Schickard, north	9		0.10	0.087	0.078
	" , south	7		0.11		0.099

Footnotes: (a) - Dzhapiashvili[15] as corrected by Markov[14]

(b) - Fedoretz[5] as derived by Markov[14]

The first feature to be noted in Figs. 17 and 18 is the marked tendency of the curves for larger particles to lie higher in the diagram. Second, the curves for opaque particles of a given size tend to lie higher than those for semi-transparent particles. But basalt is not distinguishable from greenstone (both opaque) and granodiorite is not distinguishable from tektite (both quite translucent). It seems composition is important only insofar as it affects particle opacity. Third, if the lunar measurements are valid and if our measurements correspond to lunar measurements (i.e., if no further instrumental corrections need be made), then we may conclude that opaque (or translucent) particles larger than about 50 (or 100) μ are not abundant in the lunar surface layer, except possibly in ray craters. Fourth, independent of the absolute calibration of our measurements, the relative placement of lunar values suggests that real particle-size differences must occur on the moon. In particular, since seas and crater seas are so similar in albedo and geology (if one believes in lava flows), it may be that crater seas are covered by relatively fine-grain dust. If this were so, it would surely have implications for the erosion processes operative on the moon.

An Alternate Index of the Polarization

While our measurements indicate that it should be possible to interpret lunar measurements of the maximum degree of polarization P_+ and albedo A_n in terms of sizes and opacities of particles in the dust layer overlying various lunar features, there are a number of reasons why the use of P_+ as an index of polarization is not satisfactory:

1. For a precision determination of P_+, a detailed analysis must be made of the shape of the polarimetric function in the vicinity of the maximum. As a result of the unknown shape of the polarimetric function near its maximum, a large number of data are needed near some particular phase of the moon which is different for each lunar feature that is to be studied.

2. For the very interesting central region of the moon to which the first moon probes have been and will be sent, the value of P_+ is not accessible because typically $\alpha_+ = 110°$.

3. An absolute determination of the degree of polarization must be made for which, typically, a difficult instrumental calibration must be obtained. Furthermore, corrections for atmospheric effects should be made. In practice, the atmospheric correction is ignored and measurements are confined to instruments for which the instrumental correction is as small as possible or presumably zero.

For these reasons, it is clear that a better index of the polarization effects must be sought as follows:

1. One should know the shape of the polarimetric function so that a minimum number of data points is required.

2. The index should be derived for $\alpha < 90°$.

3. One should require relative measurements only.

4. The index should manifest particle-size effects.

Consider, then, the polarization measurements obtained by T. Gehrels[12] in 1959 and replotted in the same form as Figs. 9-16 in Figs. 20-24. In each figure, certain points occur twice because they are transposed to the curve of opposite phase. The data allow two conclusions. First, it is clear that the transposed points lie essentially on the same curve as the observed points. The experimental uncertainties are given by the radii of the observed points. Second, the curve fitting the data from $\alpha = 22°$ to $\alpha = 60°$ (and sometimes to 70°) follows a straight line. This feature of Figs. 20-24 is also present in Figs. 9-16, where the relatively greater precision makes it possible to detect minute departures from a straight line. Nevertheless, it is definitely the case that the plot of the polarization data for $22° < |\alpha| < 60°$ is very straight and featureless.

We therefore propose to show that the slope of the polarization curve on $22° < |\alpha| < 60°$ is a suitable index of particle-size effects. It is clear that the slope of a straight line in the above interval satisfies the first three requirements immediately. Such an index is particularly suitable for our data in that the angular range for $\epsilon = 60°$ avoids angles of incidence far from normal incidence (asymmetric light source), the "noise" of the facet effect is negligible in the proposed angular region in comparison to the noise in the region of maximum polarization, and the nearly constant shift of the $\epsilon = 60°$ curve due to aligned bombardment tends to subtract out.

The index which we will actually use we will term "PR", the Polarization Rise from $\alpha = 20°$ to $\alpha = 60°$. The slight departure from linearity of the polarimetric function near 20° has a negligible effect on the index.

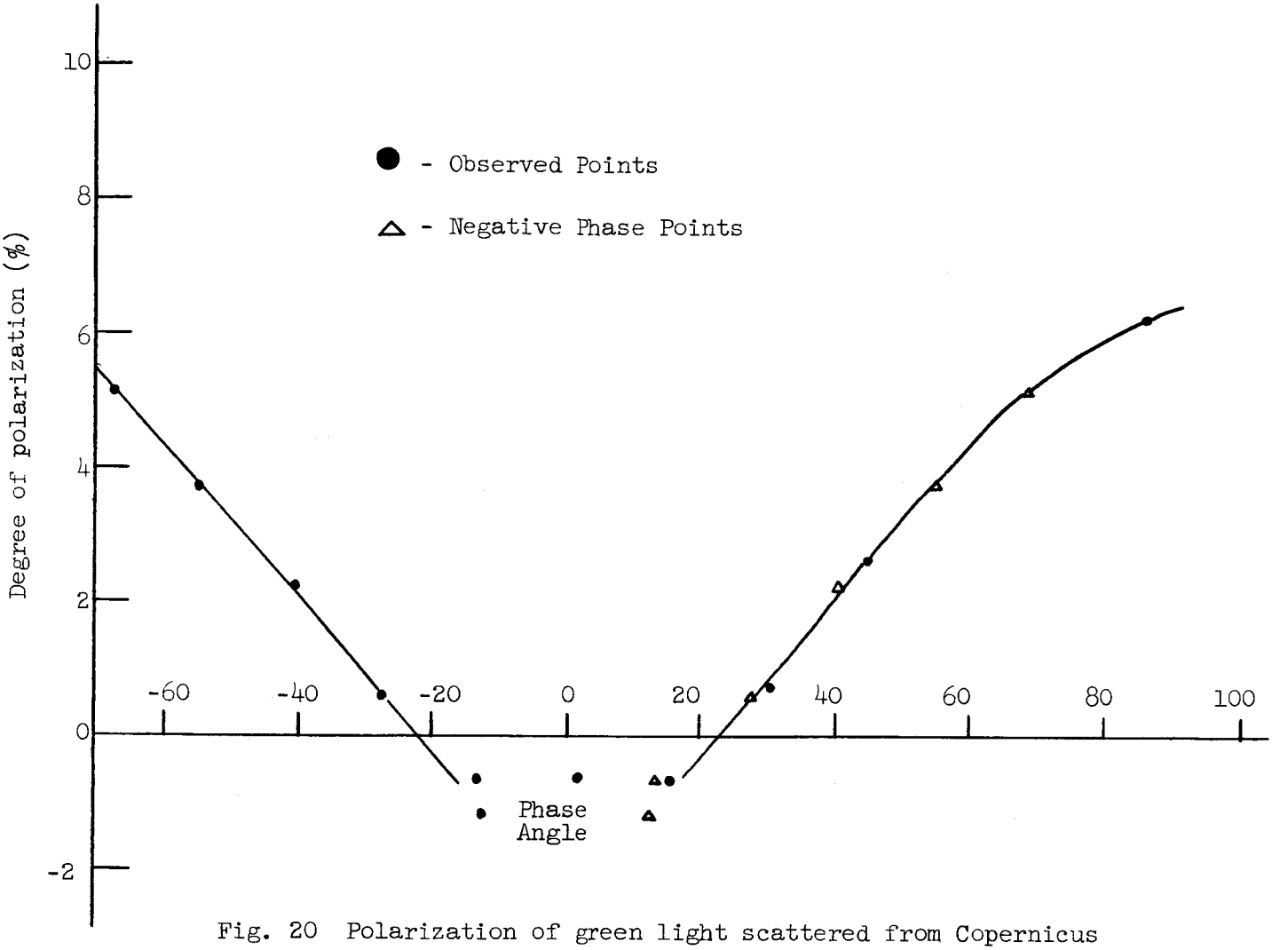

Fig. 20 Polarization of green light scattered from Copernicus NNW of central peak, from Gehrels et al., April 1959. (-20°08' ± 06', +10°11' ± 03')

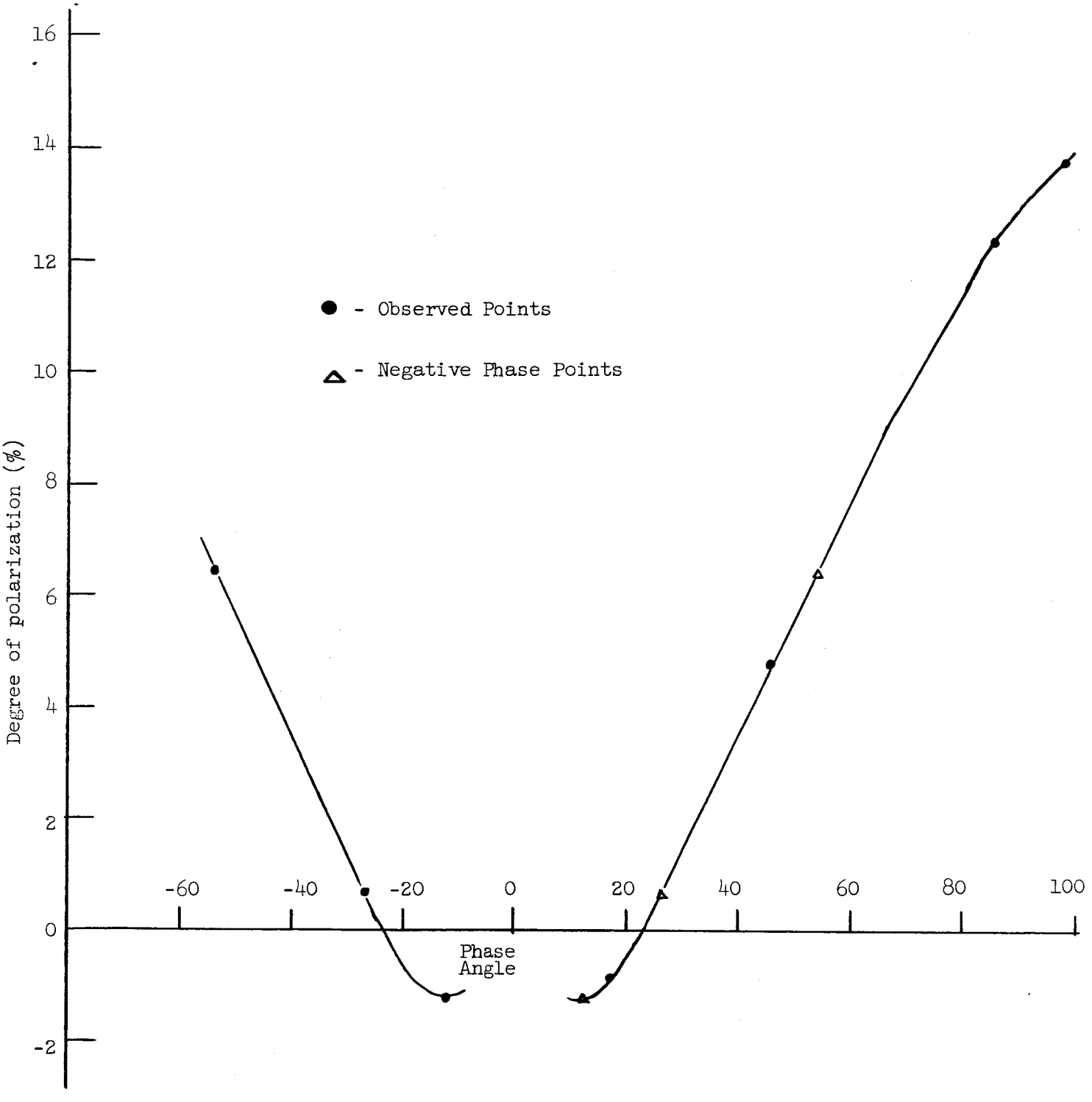

Fig. 21 Polarization of green light scattered from Mare Imbrium near the Straight Range, from Gehrels et al., April 1959. (-17°44' ± 12', +46°08' ± 05')

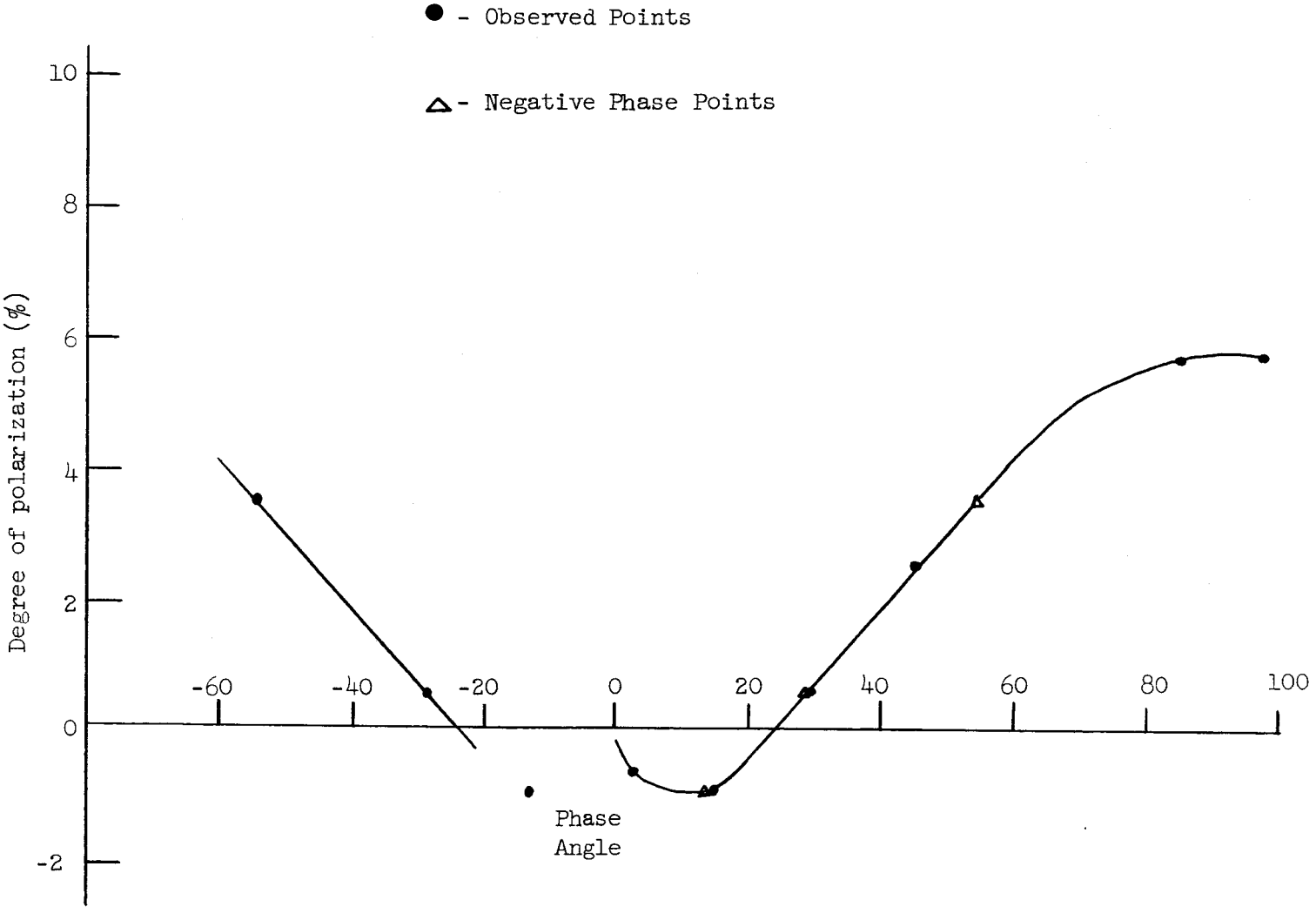

Fig. 22 Polarization of green light scattered from Clavius, between B and D, from Gehrels et al., April 1959. (-10°59' ± 02', -57°36' ± 04')

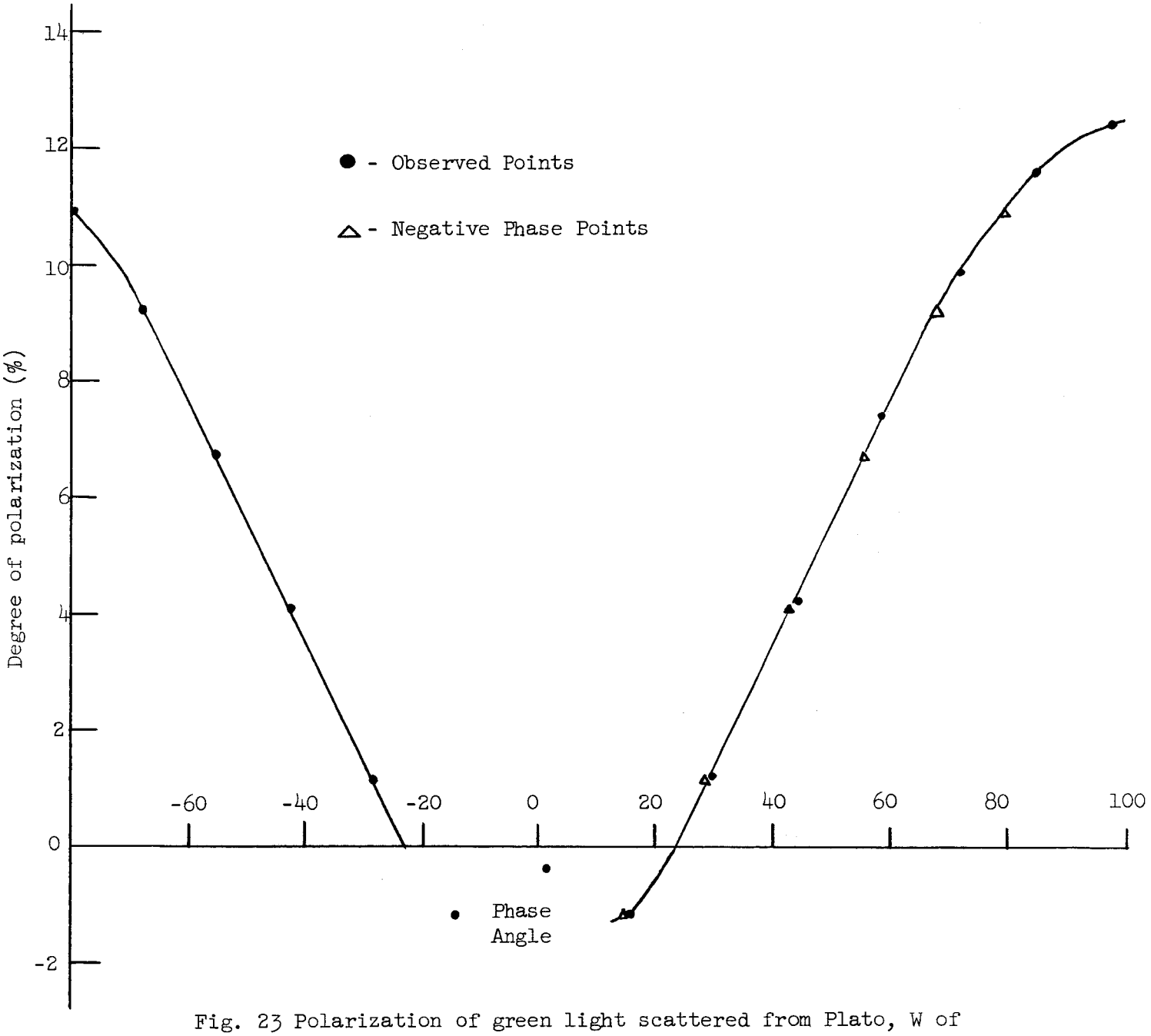

Fig. 23 Polarization of green light scattered from Plato, W of center, from Behrels et al., April 1959.
(-10°32' ± 06', +51°25' ± 03')

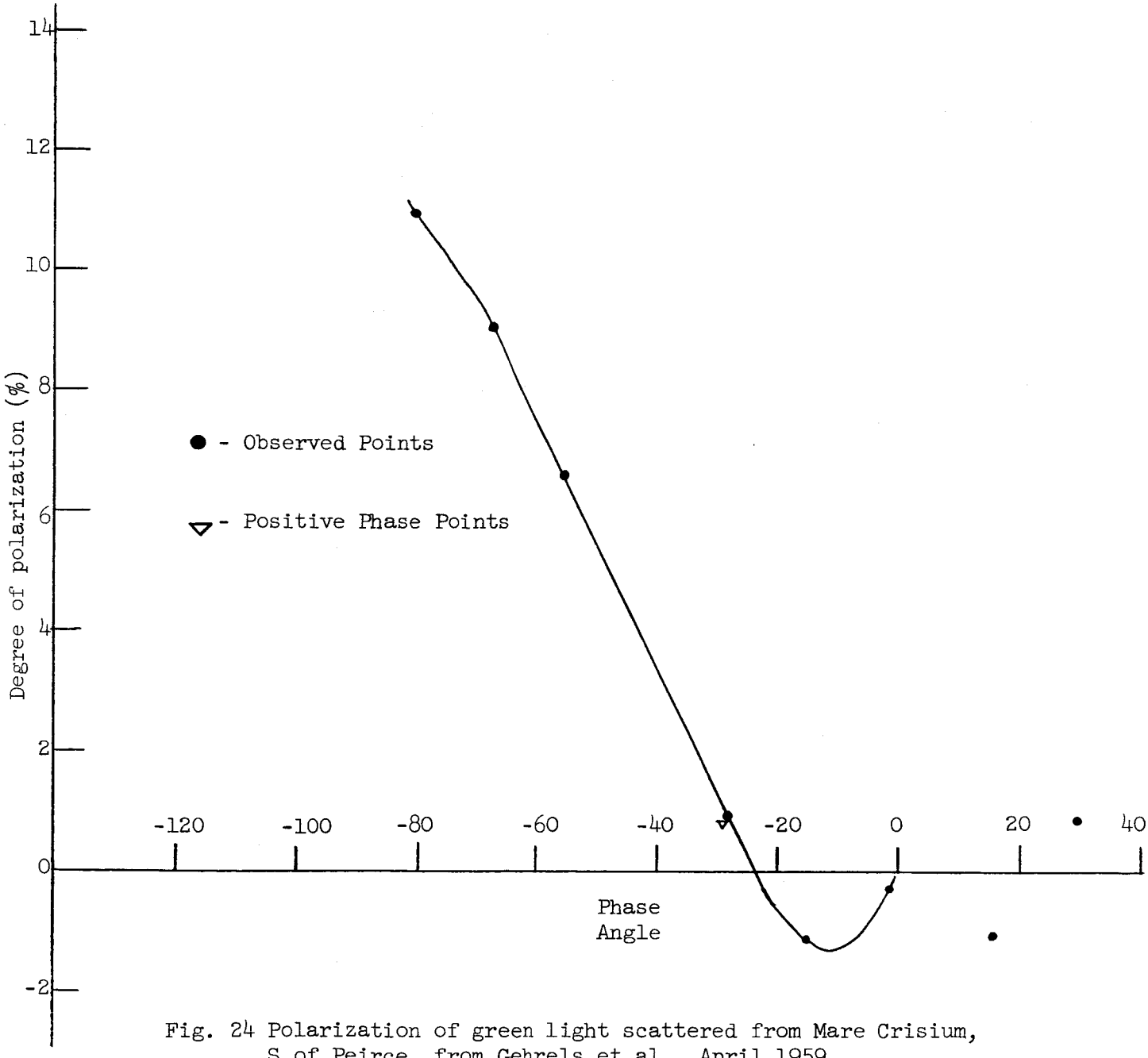

Fig. 24 Polarization of green light scattered from Mare Crisium, S of Peirce, from Gehrels et al., April 1959.
(+52°43' ± 07', +17°18' ± 06')

Analysis again will be confined to data for $\epsilon = 60°$. Comparison will be made to the lunar data of Figs. 20-24 and to the measurements of Lyot[4] on integral moonlight.

The values we have obtained for the polarization index PR for green light that was scattered from powders of tholeiitic basalt, granodiorite, greenstone, and tektite of four size ranges are given in Table II and plotted in logarithmic coordinates vs normal albedo in Figs. 25 and 26. As in Figs. 17 and 18, the points for different albedos of a given sample fall on a nearly straight line and all the lines have about the same slope. One difference from the earlier figures is the smaller slope of the lines; assumption of $PR = k\, A_n^{-m}$ implies $m = 0.8 \pm 0.1$ in comparison to $m \cong 1.3$ in the earlier analysis. One may therefore expect that the ratio P_+/PR has an albedo dependence that accounts for the difference and that, in fact, P_+ increases relative to PR as the albedo decreases. Such a dependence is obvious in Figs. 9-16 and is studied further below. The increase of P_+ relative to PR is basically the result of the increase of α_+ relative to the phase angle 60° entering PR.

It is clear from Figs. 25 and 26 that the polarization index PR is just as successful as P_+ in revealing the size of the scattering particles. Again the curves for the largest particles lie highest in the diagram. Again the opaque materials (greenstone and basalt) are very similar and the translucent materials (tektite and granodiorite) are similar, but the opaque and translucent materials are different from each other by a factor of roughly 1.2.

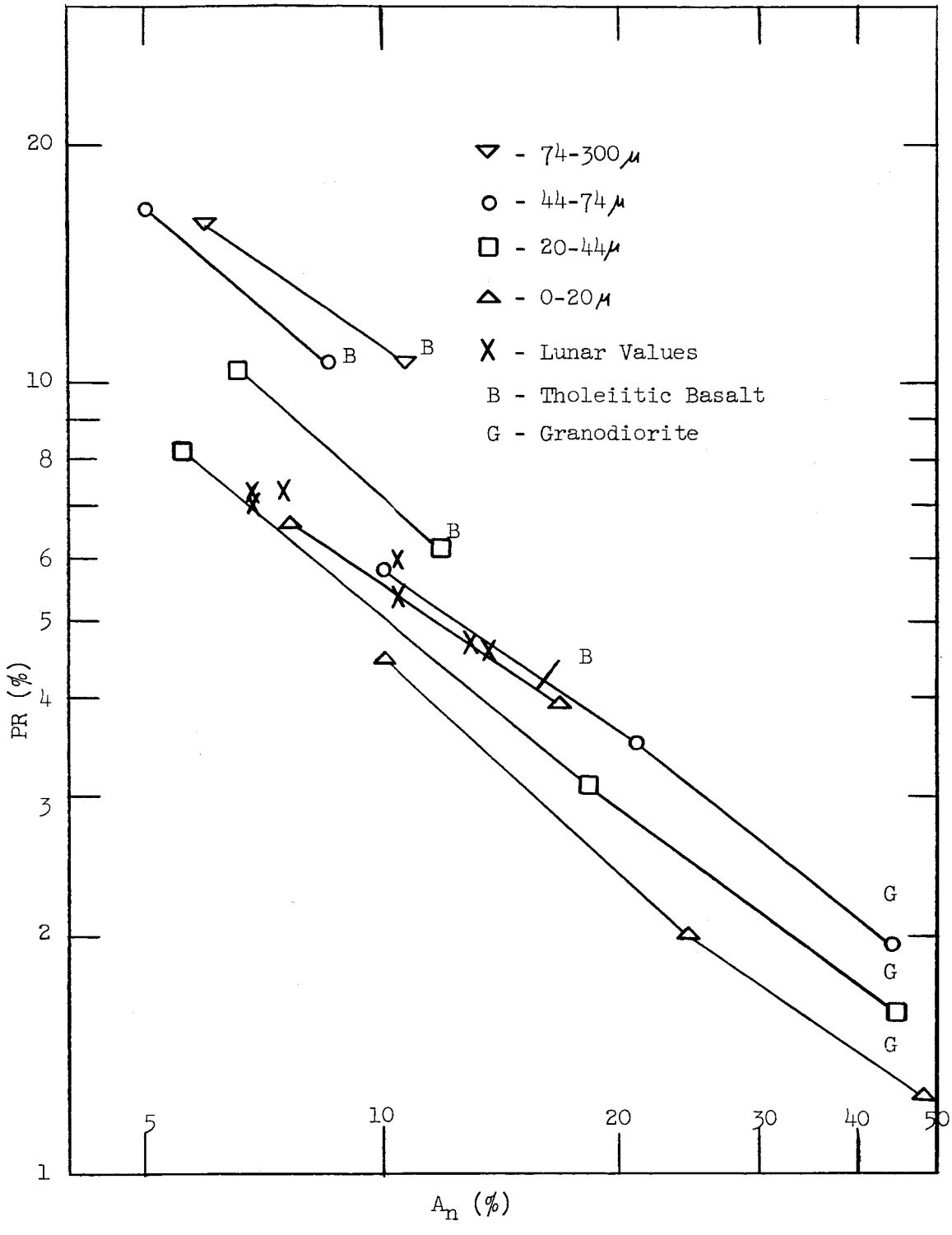

Fig. 25 Effect of particle size upon the polarization index PR for basalt and granodiorite powder.

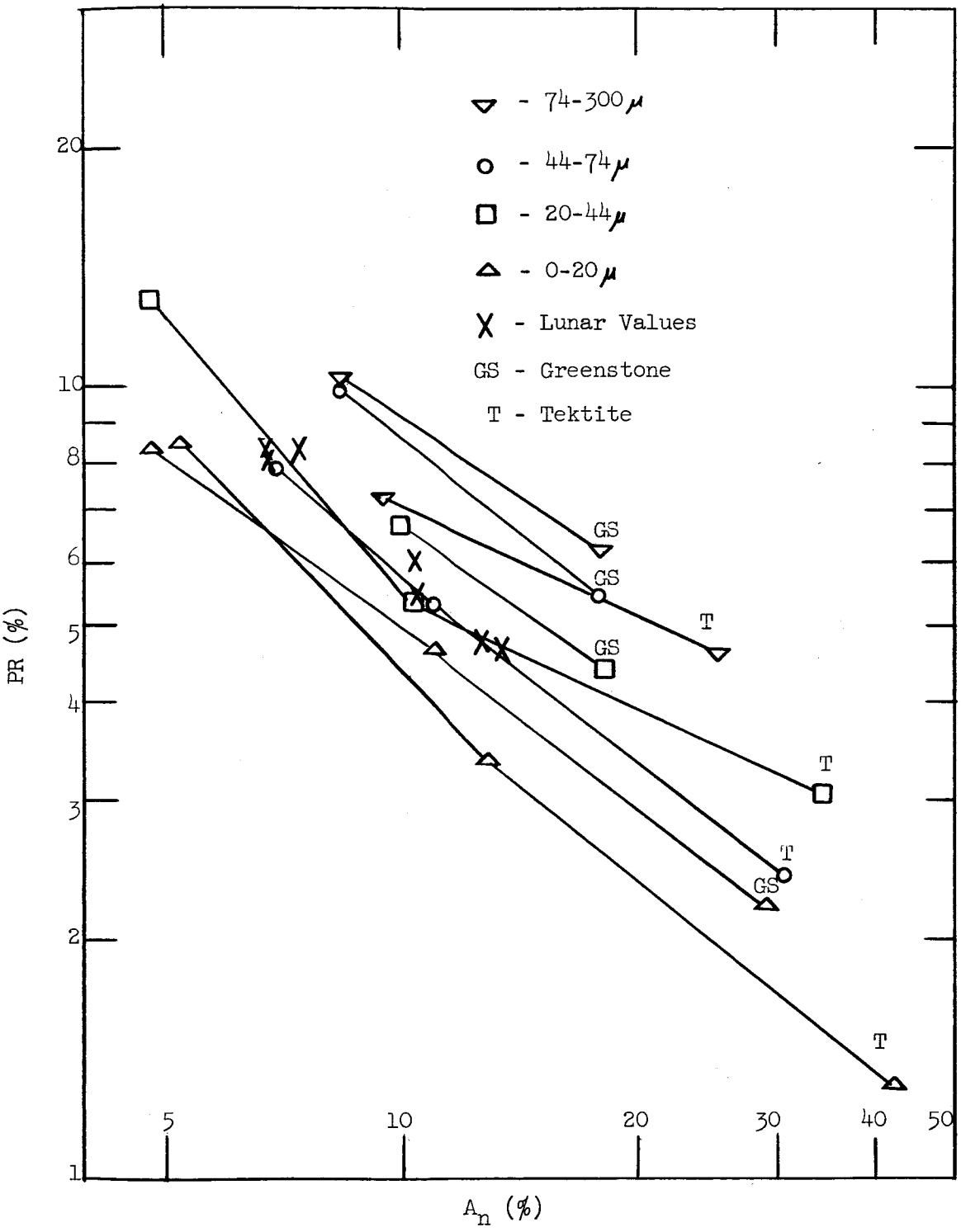

Fig. 26 Effect of particle size upon the polarization index PR for greenstone and tektite powders.

A few lunar values are given in Figs. 25 and 26 for comparison. The indices PR were read off Figs. 20-24 and the published curve of Lyot[4] for integral moonlight. The uncertainty in the PR values for the moon probably does not exceed 2%. The uncertainty in our measured PR indices is 1 to 2%. Since the spread in PR values amounts to a factor of 2, the uncertainty in PR is trivial.

Our "albedo" coordinate is fairly precise in absolute value. The "normal albedo" which we plot is actually the relative brightness of our sample and of a standard smoked MgO surface at a phase angle of 2.5°. No extrapolation of the photometric function to zero phase angle was attempted. Any extrapolation is pointless without a detailed study of the instrumental effect of finite detector angle and without a good knowledge of the shape of the (corrected) photometric function for each sample and also for the reference surface. Such an extrapolation is unmerited in a general survey in any case because the extrapolation will affect the relative normal albedos of different samples only minutely and will simply change the absolute value of the normal albedo for every sample by a nearly constant factor. From our previous section on studies of the photometric function of our samples, we estimate that our relative brightnesses should be multiplied by a factor of 1.05 to give true normal albedos.

The uncertainty in the normal albedos of the lunar features seems to be much more serious. The relative brightness of lunar features for accessible phases is, of course, well known because it can be obtained from photographs. But the absolute brightness requires, in general,

photoelectric methods and elaborate correction procedures for instrumental and atmospheric effects. Since zero phase angle for the moon cannot be observed from the earth, a final extrapolation is required. The result of such a program led Gehrels et al.[2] to normal albedos that are nearly twice the values quoted on the basis of photographic measurements in the papers of van Diggelen[5] and Sytinskaya[6] (see Appendix). We are uncertain about the validity of the extrapolation procedure of Gehrels et al. so we preferred to normalize the brightness of the lunar features observed by them to albedos quoted by van Diggelen and Sytinskaya. As listed in Tables III and IV, the latter authors agree that the normal albedo of Plato is 0.068. Accepting this albedo for Plato (with the reservation that it may be too low), the albedos for the other regions studied by Gehrels et al. were calculated from their relative brightnesses, plotted in Figs. 25 and 26, and listed in Table IV. These derived albedos are in good agreement with the albedo values of van Diggelen and Sytinskaya, as might be expected in view of the accuracy of relative brightness measurements. In fact, if we follow the same weighting procedure as prescribed by Gehrels et al. and derive a mean albedo for the whole moon, we obtain 0.105 from their values. This same value was quoted by Russell[7] and accepted by van Diggelen. It is this value for the albedo of the whole moon that we use in plotting the indices PR appropriate to the measurement of Lyot on the polarization of light from the whole moon. Actually, a slightly lower albedo would be appropriate for the eastern half of the moon because of the preponderance of maria there, and the opposite holds for the western half.

Table IV

Normal Albedos of Selected Lunar Regions for Which the Polarization Parameter PR is Available

Region	Visual[Ref.2] Brightness $\alpha = 0°$	(Ref.4) A_n	(Ref.11) A_n	(a) A_n	PR[Ref.2] (%)
Copernicus	2.09 ± 0.05	0.114	0.120	0.129 ± 0.003	4.7 ± 0.1
Mare Imbrium	1.21		0.054-0.074	0.075	8.3
E of Clavius D	2.21	0.137		0.137	4.6
Center of Plato	1.10	0.068	0.068	0.068	8.3
Mare Crisium	1.10:		0.062	0.068	8.05
Whole Moon	1.695	0.105[Ref.4, 12]		0.105	E6.0 (Ref.10) W5.4

(a) Derived from Gehrels et al.[2] as explained in text.

A value which is particularly uncertain is indicated by a colon (:).

In that case, the lunar values in Figs. 25 and 26 lie essentially on one straight line having a slope equal to the mean slope of our measurements.

If these lunar measurements are representative and if the lunar albedos are not grossly too low, then Figs. 25 and 26 agree with Figs. 17 and 18 in implying that lunar surface particles are less than 50μ in size if opaque or are less than 100 μ in size if translucent before ion bombardment. If the lunar normal albedos are to be revised upward by some factor between 1 and 2, the lunar particles are larger. The effect on lunar particle size of such a revision is roughly the same for either polarization index, P_+ or PR. Lunar particles would in that case correspond to our largest size range, 74-300μ.

Finally, we plot the ratio of polarization indices P_+/PR as a function of albedo in Fig. 27 for the four size ranges and the four materials. Except for the largest particles, the ratio P_+/PR tends to higher values as albedo decreases. There is some tendency for the smaller particles to have a lower value of the ratio, but the scatter is so great that one is led to suppose that the variation in the shape of the polarization curve expressed by P_+/PR is caused by albedo alone and not by particle size. The variation in shape as albedo decreases amounts to an increase in the upward slope of the polarization curve (expressed by PR) plus an increase in the phase angle α_+ of the maximum. For the largest particle size range that we have studied, the powder is self-compacting under atmospheric conditions and the earth's gravitational force. Probably the very large values of the ratio P_+/PR for these largest particles is partly the result of specular enhancement of the

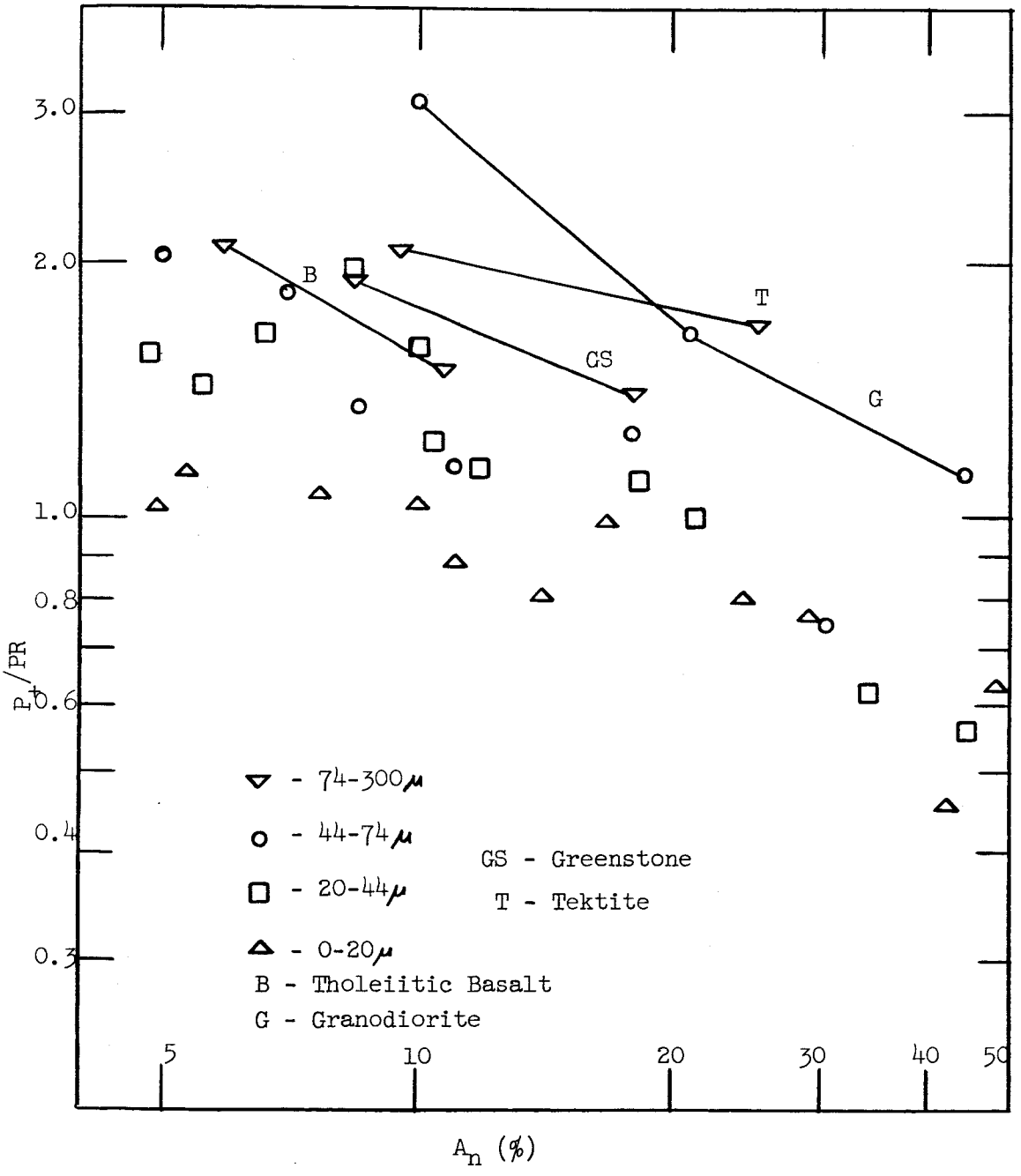

Fig. 27 The effect of particle size upon the ratio of polarization indices P_+/PR for various sifted powders of graded sizes.

polarization of light scattered diffusely in the forward direction. Under the lunar conditions of low gravity and such an excellent vacuum that inter-particle forces can be far greater, a powder corresponding to our largest size range might not be self-compacting.

APPENDIX

DATA AVAILABLE ON MAXIMUM POLARIZATION AND ALBEDO OF LUNAR FEATURES

The French or Russian data to be discussed here are now available in English translation. The data on maximum polarization and albedo of lunar features are collected in Table III and pertain to green light.

Markov[9] first attempted in 1960 to correlate quantitatively the maximum polarization of lunar features with their corresponding albedos. He had available the polarimetric data of Dzhapiashvili[10] which, however, were uncertain in absolute magnitude because of an instrumental polarization of about 4%. Markov[11] undertook observations jointly with Myukhkyurya with an automatically recording electropolarimeter (with a polaroid rotating at high speed) designed by Myukhkyurya.[12] The instrument is less subject to instrumental errors and was used at a single lunar phase with the goal of correcting the work of Dzhapiashvili. Markov[9] then gave a table of polarization values for 41 lunar features of which 31 are given in Table III. The albedos which he gave were derived from the work of Fedoretz.[13] In 1952, Fedoretz published tables of 162 points on the moon for which he had measured the radiance, on 20 lunar plates, taken at different phase angles. In 1958, van Diggelen[5] published his very complete study of the photometric properties of lunar crater floors. But in comparing his measured radiances to that of Fedoretz, he found a disturbingly large scatter of points about a linear curve, amounting to a factor of 2. In our comparison of the albedos given

by van Diggelen and by Markov as listed in Table III, we find that the albedos derived by Markov need to be multiplied, on the average, by a factor of 0.77 to bring them into agreement with the values given by van Diggelen. Van Diggelen compared his albedos to a catalog of albedos published in 1953 by Sytinskaya.[6] He found excellent agreement with the earlier catalog and suggested that his values need be multiplied only by a factor of 0.972 to agree in the mean. It seems probable, therefore, that the albedo values of van Diggelen and Sytinskaya are more reliable than those derived by Markov. The albedos given by Markov were not used in Fig. 19.

A small amount of additional polarization values are available from the early determinations of Lyot[4] and from the recent, short work of Clarke.[8] Most of the measurements of Lyot pertain to regions whose coordinates are poorly known so that reliable albedos are difficult to obtain. The work of Clarke was devoted more to the wavelength dependence of polarization than to a survey of maximum polarizations. The overlap of polarization data from different observers is negligible, the single case in Table III, Sinus Iridum, being such a large region (having varied colors) that the poor agreement might be expected. It is to be hoped that far more polarization data will be obtained and that the observers will tabulate their determinations for various phases.

IV. LIST OF REFERENCES

1. Litton Systems, Inc. Applied Science Division. Report No. 2722. Investigation of sputtering effects on the moon's surface, by G. K. Wehner, D. L. Rosenberg, and C. E. KenKnight. Contract NASw-751. Seventh quarterly status report (October 25, 1964-January 24, 1965).

2. Gehrels, T., T. Coffeen, and D. Owings. Wavelength dependence of polarization. III. The lunar surface. Astron. J. 69: 826-52 (1964).

3. Litton Systems, Inc. Applied Science Division. Report No. 2669. Investigation of sputtering effects on the moon's surface, by G. K. Wehner, D. L. Rosenberg, and C. E. KenKnight. Contract NASw-751. Sixth quarterly status report (July 25-October 24, 1964).

4. Lyot, B. Research on the polarization of light from planets and from some terrestrial substances. Ann. Observatoire de Paris, Section de Meudon 8, No. 1 (1929). (NASA Technical Translation F-187).

5. van Diggelen, J. Photometric properties of lunar crater floors. Rech. Astron. Observ. Utrecht 14, No. 2 (1958). (NASA Technical Translation F-209).

6. Sytinskaya, N. N. Catalog of the absolute values of visual reflectivity of 104 lunar formations. Astron. Zh. 30: 295-301 (1953).

7. Russell, H. N. Astrophys. J. 53: 114 (1916).

8. Manchester, University. Department of Astronomy. Observations of the frequency dependence of polarisation of the light of the moon and of Mars, by D. Clarke. Contract AF 61(052)-378. Technical Note No. 3 (January 13, 1964). AD 602,668.

9. Markov, A. V. Polarization properties of the lunar surface. In Barabashov, N. P. et al. The moon. Moscow, State Publishing House of Physics-Mathematical Literature, 1960. (U. S. Air Force. Aerospace Intelligence Center. Translation MCL-882. AD 261,784. pp. 209-31).

10. Dzhapiashvili, V. P. Study of the polarization properties of formations on the lunar surface by means of electrophotometric measurements. Byul. Abastumani Astrofiz. Observ., No. 21: 168 (1957).

11. Markov, A. V. Results of experimental studies of the polarization of features of the lunar surface. Izv. Astron. Observ., Pulkovo (USSR) 20, No. 158: 138 (1958).

12. Myukhkyurya, V. I. An electrophotometer for measuring the intensity of polarization of light. Issled. Oblakov Osadkovi Grozovogo Elektrichestva, No. 5: 139 (1957).

13. Fedorets, V. A. Photographic photometry of the lunar surface. Tr. Astron. Observ. Khar'kovsk. Univ. 2, 10: 49-172 (1952).